

Singapore Management University

## Institutional Knowledge at Singapore Management University

---

Research Collection Lee Kong Chian School Of  
Business

Lee Kong Chian School of Business

---

1-2019

### **Swaption portfolio risk management: Optimal model selection in different interest rate regimes**

Poh Ling NEO

Chyng Wen TEE

*Singapore Management University*, cwtee@smu.edu.sg

Follow this and additional works at: [https://ink.library.smu.edu.sg/lkcsb\\_research](https://ink.library.smu.edu.sg/lkcsb_research)

 Part of the [Finance and Financial Management Commons](#), and the [Portfolio and Security Analysis Commons](#)

---

#### Citation

NEO, Poh Ling and TEE, Chyng Wen. Swaption portfolio risk management: Optimal model selection in different interest rate regimes. (2019). *Journal of Derivatives*. 1-27. Research Collection Lee Kong Chian School Of Business.

Available at: [https://ink.library.smu.edu.sg/lkcsb\\_research/6404](https://ink.library.smu.edu.sg/lkcsb_research/6404)

This Journal Article is brought to you for free and open access by the Lee Kong Chian School of Business at Institutional Knowledge at Singapore Management University. It has been accepted for inclusion in Research Collection Lee Kong Chian School Of Business by an authorized administrator of Institutional Knowledge at Singapore Management University. For more information, please email [libIR@smu.edu.sg](mailto:libIR@smu.edu.sg).

# Swaption Portfolio Risk Management: Optimal Model Selection in Different Interest Rate Regimes

Poh Ling Neo\* Chyng Wen Tee<sup>†‡</sup>

## Abstract

We formulate a risk-based swaption portfolio management framework for profit-and-loss (P&L) explanation. We analyze the implication of using the right volatility backbone in the pricing model from a hedging perspective, and demonstrate the importance of incorporating stability and robustness measure as part of the calibration process for optimal model selection. We also derive a displaced-diffusion stochastic volatility (DDSV) model with a closed-form analytical expression to handle negative interest rates. Finally, we show that our framework is able to identify the optimal pricing model, which leads to superior P&L explanation and hedging performance.

**Keywords:** *derivatives valuation, interest rate markets, swaptions, risk management, portfolio management, pricing and hedging, stochastic volatility models, SABR model.*

---

\*School of Business, Singapore University of Social Science, 463 Clementi Road, Singapore 599494. Tel: +65 6248 0393. Email: [p1neo@suss.edu.sg](mailto:p1neo@suss.edu.sg). Poh Ling Neo's work was funded by a research grant from the Centre of Applied Research, Singapore University of Social Sciences.

<sup>†</sup>Lee Kong Chian School of Business, Singapore Management University, 50 Stamford Road #05-01, Singapore 178899. Tel: +65 6828 0819. Email: [cwtee@smu.edu.sg](mailto:cwtee@smu.edu.sg).

<sup>‡</sup>The authors would like to acknowledge the comments and suggestions from an anonymous referee, which lead to much improvement in the flow and clarity of this paper.

# 1 Introduction

What are the defining characteristics of an optimal model from a pricing and hedging standpoint? For practitioners, a good model should:

1. match market dynamics by capturing the right risk factors
2. reproduce market prices of liquid instruments after calibration without any “fudge” factors
3. have robust and stable model parameters
4. have Greeks that can explain daily profit-and-loss (P&L) movements

In this paper, we show how to use these guidelines to select the optimal pricing model for the swaption market, and demonstrate that the holistic approach of taking robustness, Greeks, and P&L explanation as part of the calibration process can lead to superior hedging performance.

Swaptions are the main interest rate volatility instrument in the fixed income market, and are traded in high volume between inter-dealers and institutional investors to hedge interest rate volatility exposure, or to take on positions on yield curve movements. In addition to being the main instrument for interest rate risk management, they also form the basis for all volatility-sensitive interest rate product valuations, including Bermudan swaptions, callable swaps, constant maturity swap (CMS) payoffs, and yield-curve spread options, to name a few. Therefore, efficient risk management of swaption portfolio plays a crucial role across the whole spectrum of interest rate volatility products.

Standard market practice is to use the stochastic-alpha-beta-rho (SABR) model to risk manage swaption portfolio. This paper highlights the importance of selecting the optimal pricing model, including the right volatility backbone, for efficient risk management. We formulate an intuitive profit-and-loss (P&L) explanation framework that decomposes daily portfolio value movement into hedgeable Greeks components. In addition to fitting to market prices, we show that the stability of Greeks and sensitivity, along with the economy of P&L explanation, can also be used to determine the optimal model. Using the Eurozone (EUR-denominated) swaption market as a case study, we further demonstrate that using SABR model to risk manage swaption portfolio could be problematic as swap rates or strikes become negative. To resolve this problem, we formulate a displaced-diffusion stochastic volatility model for swaption pricing that retains the analytical tractability and computational efficiency of the SABR model. The displaced-diffusion dynamic for the swap rate process can handle negative rates or strikes without any further ad hoc adjustment.

It has long been established that the swaption market follows neither normal or lognormal backbone,

but a mixture of the two. Swaption portfolio managers heuristically select the value of the  $\beta$  parameter in their SABR model based on subjective perception of the prevailing backbone behavior, and calibrate the rest of the model parameters ( $\alpha$ ,  $\rho$ , and  $\nu$ ) to match the swaption prices observed in the market. In high interest rate environments, portfolio managers tend to assume that rates are closer to being lognormally distributed ( $\beta \rightarrow 1$ ), while in low interest rate environments, the rates are closer to being normally distributed ( $\beta \rightarrow 0$ ). Fixing a constant beta, or equivalently making an assumption on the underlying distribution, such as a normal or lognormal, cannot fully capture market risk.

As mentioned earlier, when determining the optimality of a pricing model, standard market practice is to check how close can it fit observable market prices (or implied volatilities). However, as we will make clear in this paper, SABR model is able to fit market prices very well. In general, it is possible to obtain multiple sets of model parameters that fit the market with comparable goodness-of-fit. It is therefore advantageous to incorporate P&L explanation performance as well as model stability and robustness as part of the optimal model selection criteria. This extended model assessment framework will allow portfolio managers to avoid ambiguity and uniquely determine the optimal model for pricing, hedging, and risk management purposes. In other words, when multiple models are able to fit market prices well, the model that can explain P&L movement over time in the most concise and economical manner is superior.

Building on the insights and findings of Zhang and Fabozzi (2016), we further develop the concept of optimal hedging performance. When the swaption market moves, how should one explain the realized profit-and-loss (P&L) of one's swaption portfolio? From a practitioner's perspective, it is most insightful to explain the changes of a portfolio value by attributing them to contributions from 1) movement in rates (interest rate delta), 2) movement in at-the-money (ATM) implied volatility (interest rate vega), 3) movement in implied volatility skew (asymmetrical slope in implied volatility), and 4) movement in implied volatility smile (symmetrical curvature in implied volatility). To this end, we formulate a P&L explanation framework and use it as a basis to assess the robustness of the pricing models. We also introduce the concept of optimal hedging performance, measured by the "concentration" of P&L breakdown. We show that choosing the right volatility backbone yields the best hedging performance.

This paper is organized as follows: Section 2 provides a literature review of the published research in this area. Section 3 introduces the data used in this study, and presents the empirical analyses performed on the data set. To handle negative interest rate regime, a displaced-diffusion stochastic volatility model is derived in Section 4. Next, a P&L explanation framework and hedging performance benchmark are formulated in Section 5, followed by our results on the hedging performance comparison of the models.

Finally, conclusions are drawn in Section 6.

## 2 Literature Review

A key question swaption portfolio managers face is whether the swap rates follow a “normal” or a “lognormal” model. This is an important question, as the model dynamic also determines the backbone of the swaption implied volatility surface, which in turn affects how swaption prices change in response to rate movements. Several recent studies have investigated this subject extensively. Levin (2004) explores the swaption market and demonstrates that swaptions with low strikes are traded with a close-to-normal volatility ( $\beta \rightarrow 0$ ), while swaptions with higher strikes are traded with a square root volatility ( $\beta = 0.5$ ). Deguillaume, Rebonato and Pogudin (2013) look at the dependence of the magnitude of rate moves on the rate levels, and discover a universal relationship that holds across currencies and over a very extended period of time (almost 50 years). Interestingly, they found that volatilities of very low and very high rates behave in a lognormal fashion, while intermediate rates exhibit normal behavior. More recently, Meucci and Loreanian (2016) show that US Treasury (UST) yields and Japanese Government Bond (JGP) yields are also neither normal nor lognormal. Using the “shadow rate” concept introduced by Black (1995), they develop an “inverse-call” method to convert observable interest rates into shadow rates. They then show that these shadow rates have superior quality from a risk management perspective, in that the behavior is relatively more consistent whether rates are low or high.

In the fixed-income market, the stochastic alpha-beta-rho (SABR) model proposed by Hagan et al. (2002) is the de facto model used for swaptions pricing. Compared to other stochastic volatility models (say, for instance, the Heston (1993) model), the main advantage of SABR model lies in its ability to express implied volatility as a closed-form analytical formula, allowing swaptions to be priced in a quick and efficient manner. Being able to value swaption portfolio efficiently using analytical formula is vital, as swaptions are used as the basis to price exotic volatility products. For instance, pricing CMS payoffs involve computing a one-dimensional integral across a continuum of weighted swaptions (see Brigo and Mercurio (2006) and Andersen and Piterbarg (2010) for more information). Having an analytical expression for the swaption prices significantly speed up the pricing speed of exotic products.

The performance of SABR model has been investigated extensively in the literature. Wu (2012) explore the application of SABR model to the interest rate cap market. The study concludes that SABR model exhibits excellent pricing accuracy and captures the dynamics of the volatility smile over time very well. Separately, Yang, Fabozzi and Bianchi (2015) apply SABR model to the foreign exchange

market. They use empirical methods to show that SABR model can fit market option prices and predict volatility well. SABR model is also useful in analyses involving volatility risk premia. For example, Duyvesteyn and de Zwart (2015) use SABR model to test and analyze the maturity effect in the volatility risk premium in swap markets by looking at the returns of two long-short straddle strategies.

Given the wide-spread use of SABR model in the risk management of interest rate derivatives, Zhang and Fabozzi (2016) investigate the importance of choosing the right volatility backbone under SABR model, and how an optimal choice of the  $\beta$  parameter leads to superior hedging performance by minimizing pricing error. The key to the proposed method is that the option pricing model parameters not only can be estimated by calibrating the model to the market implied volatility smile, but also can be estimated by choosing the set of parameters that minimize the hedging error. The proposed method meets the no-arbitrage condition, delivering better hedging performance than the existing fixed-beta style calibration method.

It is important to note that the process in SABR model specified for the forward swap rate follows a constant elasticity of variance (CEV) process introduced by Cox and Ross (1976) (see Section 4 and Cox (1996) for further information). However, unless we are explicitly setting  $\beta = 0$ , the model cannot support negative rates or strikes. Practitioners circumvent this problem by either using a normal SABR model with  $\beta = 0$ , or a shifted SABR model that moves both the rates and the strikes up by a pre-determined fixed positive amount. Apart from these ad hoc fixes, more sophisticated solutions have also been recently proposed. Anthonov, Konikov and Spector (2015a) formulated a free boundary SABR model by providing a structure to remove the negative rates boundary, making it flexible in terms of calibration to market data. Anthonov, Konikov and Spector (2015b) also propose method to handle negative rates by mixing zero-correlation free boundary SABR model with a normal SABR. However, these models are more complex to evaluate, and could be challenging to calibrate.

A good alternative model to handle negative rates is to use the displaced-diffusion dynamic proposed by Rubinstein (1983). This parameterization can be interpreted as a simple linearization of the CEV dynamics around the initial value of the underlying. Similar to the CEV model, a displaced-diffusion model implies that the forward rate behaves more like a normal distribution when rates are low, and vice versa. Unlike CEV model, negative rates are admissible in a displaced-diffusion model. This coincides with the recent observation that interest rates have not only been negative but distributed more like a normal distribution. In fact, Marris (1999) shows that there exists a close correspondence between the CEV and the displaced-diffusion dynamics, and that, once the two models are suitably calibrated, the resulting interest rate option prices are virtually indistinguishable over a wide range of strikes and

maturities. Joshi and Rebonato (2003) therefore use the displaced-diffusion setting, which, unlike the CEV case, allow simple closed-form solutions for the realization of the forward rates after a finite period of time, as a computationally simple and efficient substitute for the theoretically more pleasing CEV framework, which does not allow negative forward rates. In fact, Svoboda-Greenwood (2009) posited displaced-diffusion processes as suitable alternatives to a lognormal process in modelling the dynamics of market variables such as stock prices and interest rates. The mathematical properties of a displaced-diffusion model is rigorously investigated further in Lee and Wang (2012).

Observation in the recent negative interest rate regime in the Eurozone shows us that zero rate did not become an absorbing barrier, contrary to the behavior of a CEV process with  $\beta \in (0, 1)$ . On the other hand, rates did become negative, but there appears to be a lower bound as to how negative it can be, which is controlled by the European Central Bank (ECB) (see Siegel and Sexauer (2017) for further discussions from the economic aspect). These rate behaviors are consistent with the characteristics of a displaced-diffusion dynamics, as opposed to a normal model which does not have a theoretical lower bound. Recent use cases of displaced-diffusion model include Chen, Hsieh and Huang (2018) to resolve severe problems of the existing Libor Market Model (LMM) that has failed since 2008 crisis. In Section 4 we derive a displaced-diffusion stochastic volatility model with closed-form analytical expression for swaption pricing, and show that it is also able to match market prices as well as SABR model, but does not required any ad hoc fixes to handle negative rates.

### 3 Data and Empirical Analyses

The swaption data used in this study is acquired from IHS Markit. The swaptions are denominated in EUR. IHS Markit collects market data quotes from all data vendors and subject the data to specifically designed checks before cleaning and collating them into aggregated data in daily frequency. The data used in this paper covers 5 full calendar years from 1-Oct-2012 through to 30-Sep-2017, with 1,305 trading days. The data on each day comprises of 20 expiries and 14 tenors, with 14 strikes available for each swaption chain (expiry-tenor pair), defined by their respective moneyness (from at-the-money (ATM) to  $ATM \pm 300$  basis points).

Table I provides a quick summary of the market data. Although a wide range of expiry-tenor pairs are provided by IHS Markit, they have varying degree of liquidity. To ensure the relevance of our analysis, we document and present our results for 4 highly liquid expiry-tenor pairs:  $5y10y$ ,  $10y10y$ ,  $20y20y$ ,  $30y30y$  in the paper. However, the conclusions drawn in the paper are general, and are applicable across

all expiry-tenor pairs.

Standard convention in the fixed-income market is to quote implied lognormal volatility based on the Black (1976) model. However, as swap rates become lower, and eventually enter the negative regime, swaptions with negative strikes and forward rates can no longer be quoted using the Black (1976) model, which assumes that interest rates follow a lognormal distribution. As a workaround, IHS Markit also provides implied “normal” volatility quotes based on a model assuming normal distribution, in which negative rates and strikes are admissible. On the other hand, ICAP, a major interest rate derivatives broker, continues showing implied lognormal volatility quotes, but started shifting the forward rates and strikes up by a pre-determined fixed amount since December 2012. Today, the shift amount is 3% for Euro (EUR) and 4% for Swiss Franc (CHF).

To provide a high level overview of rate levels over time, Figure 1 plots the par swap rates and forward swap rates over the 5-year period included in our analysis. The top figure shows the spot starting Euro OverNight Index Average (EONIA) 1-week overnight index swap (OIS), and the par swap rates of Euro interest rate swaps (IRS) with increasing maturities of 1y, 2y, 5y, 10y, 20y, and 30y. The bottom figure shows the forward swap rates, which are the relevant parameters used for swaption pricing. For economy of presentation, only 4 liquid expiry-tenor pairs (5y10y, 10y10y, 20y20, and 30y30y) are plotted, though the same trend and behavior are observed across the entire data set. The important economic landmark events are also labeled in the figure. The European Central Bank (ECB) cuts EUR rates to negative in June-2014, and swap rate levels started falling after that. Although short expiries swap rates only became negative after March-2015, strikes of out-of-the-money receiver swaptions (low strikes swaptions) have already become negative prior to that. From the figure, it is also obvious that the period included in the study can be split into a “moderate” rate regime (prior to June-2014) and a “low” rate regime (post June-2014).

We empirically measure forward swap rate volatility by plotting annualized standard deviation of daily increments against the rate levels. We collect all daily rate increments and group them into 4 rate levels – [0, 1%), [1, 2%), [2, 3%), [3, 4%), with each level corresponding to a specific range of rate level. After the data is grouped, we calculate the standard deviation within each group, and then annualize them ( $\times 10000 \times \sqrt{252}$  in basis point unit). Figure 2 plots the standard deviation against forward swap rate levels, along with the number of observations in each level. From the figure, it is clear that as the rate levels increase, their standard deviations decrease (solid line and right axis). This observation is fully consistent with standard swaption market practice, where portfolio managers use a SABR model with a  $\beta$  parameter closer to 1 under high rate regime, but a  $\beta$  parameter closer to 0 under low rate regime. The

bar charts (left axis) indicate the number of observation in each level. Again, for the sake of economy in presentation, we only plot 4 liquid expiry-tenor pairs, namely 5y10y, 10y10y, 20y20y, and 30y30y, but comparable result is obtained for all expiry-tenor pairs in our data set.

Apart from the standard deviation of daily swap rate movement, higher moments of the swap rate distribution such as skewness and kurtosis also have important implication on the swaption portfolio, since they directly impact the shape of the implied volatility surface. To investigate the dependence of higher moments on the rate levels, we calculate skewness to explore asymmetry in daily rate movement. The forward swap rate levels are grouped into the same 4 rate levels, and Figure 3 plots the skewness of the forward swap rate daily changes against forward swap rate levels (solid line and right axis), along with the number of observations in each level (bar charts and left axis). Skewness is negative under low rate regime, but becomes positive under high rate regime. This shows that the rates movement distribution has a heavier right tail when rates are higher, but a heavier left tail when rates are lower. Note that this statistical behavior also conforms to the observed volatility backbone property in the swaption market — normal distribution has zero skewness, while a lognormal distribution exhibits positive skewness. We also calculate the excess kurtosis of the daily swap rate movement. The forward swap rate levels are again grouped into level, and Figure 4 plots the excess kurtosis against the forward swap rate level. The excess kurtosis are all positive, highlighting the fact that the distributions of daily changes in rates have heavier tails than normal distribution. However, the tails are relatively heavier under low rates regime, and relatively lighter under high rates regime. In terms of implied volatility surface, this means that the smile profile is more pronounced during low rates regimes.

To provide a simple empirical measure of the volatility backbone, we investigate the relationship between at-the-money (ATM) implied volatilities and forward swap rates. A lognormal volatility backbone will imply the absence of any dependence between implied lognormal volatility on the rate levels, while a normal volatility backbone implies the absence of any dependence between implied normal volatility on the rat levels. Figure 5 plots the implied lognormal volatilities (top figure) and the implied normal volatilities (bottom figure) against forward swap rates. In the upper figure, it is obvious that as rates become lower, higher lognormal implied volatilities are required to match market prices. On the other hand, when rates are higher, the lognormal implied volatilities required to match the market swaption prices are lower. This inverse relationship between Black lognormal implied volatilities and forward swap rates is a clear and visual indication that the backbone of the swaption market is not lognormal — higher rates are associated with lower lognormal volatilities, and vice versa. Compared to the lognormal volatilties, the normal implied volatilities in the bottom figure are relatively flatter. This shows that the

volatility backbone of the swaption market is closer to the normal model. However, note that although lower rates are associated with a relatively flat implied normal volatilities, for higher rates the normal volatilities are moderately upward sloping. This indicates that the optimal volatility backbone is between normal and lognormal.

Next, we use principal component analysis (PCA) to investigate the factor structures of daily changes in implied volatility surface of the swaption chains. This analysis is inspired by Fan, Gupta and Ritchken (2007), who also employ PCA to the swaption market to investigate the number of factors required for yield curve models to ensure pricing accuracy. However, our analysis here focus directly on the implied volatility surface, instead of the yield curve. The objective of this PCA-based statistical volatility shape analysis is two-fold. First, we want to identify the main drivers of the shape variation in implied volatility surface, and their relative importance. Second, the characteristics of the patterns in shape variation can provide guidance to whether the pricing models has sufficient degree of freedom to capture the dynamics of the implied volatility surface. PCA analyses are generally sensitive to the units in which the underlying variables are measured. It is therefore customary to standardize variables to unit variances, or equivalently to extract the eigenvalues and eigenvectors from the correlation matrix. Figure 6 plots the first, second and third principal components before and after the negative rate regime for the 20y20y swaptions. The same observation and result are obtained for other expiry-tenor pairs. To ensure that the analysis can be run across the 5-year period included in this study, we use a 3% shifted implied lognormal volatility. We ignore the  $\pm 300\text{bps}$  strikes as these quotes are absent in a small amount ( $\approx 5\%$ ) of the dates in our dataset. We split our data into a “moderate” rate regime (Oct-2012 to Jun-2014) and a “low” rate regime (Jul-2014 to Sep-2017). Similar to the common case of yield curve analysis, the first principal component (PC) captures parallel implied volatility curve movement, the second PC captures the change in volatility skew (asymmetric slope movement), while the third PC accounts for the variation in implied volatility smile (symmetric curvature movement). The explanatory power of each PC is measured by the magnitude of the eigenvalues. The ratio of explained variance of each PC is labeled in the figure. Prior to the negative rate regime (until June-2014), the first PC alone accounts for more than 98% of the implied volatility curve movement. After entering the negative rate regime (July-2014 onward), slope and curvature play a relatively more prominent role, collectively account for  $\approx 7\%$  of the implied volatility curve movement. Nevertheless, for the entire period included in our analysis, the first three PCs together account for in excess of 99.65% of the variance. This is a strong indication that the dynamics of the SABR model has sufficient degree of freedom to capture the shape variation of the implied volatility surface, with  $\alpha$ ,  $\rho$ , and  $\nu$  corresponding to level, slope, and curvature, respectively. In the lower figure,

an abrupt drop in value is observed on the 3<sup>rd</sup> PC for the  $-200\text{bp}$  strike point, which might be attributed to illiquid data point for very low (negative) strike swaptions during the negative rate regime.

Statistical decomposition of the implied volatility curve’s daily changes described above demonstrates that there are three principal factors explaining the majority of the variation: level, slope, and curvature. Next, we perform further empirical analysis to study the variation of these three factors over time, as well as their dependence on the rate levels. We borrow the concept of proxy “empirical slope” and “empirical curvature” from the yield curve literature to provide a model-free approach to quantify skew (asymmetric) and smile (symmetric) in the implied volatilities as proxy measures of slope and curvature. In general, the level of the curve can be considered to be anchored by the at-the-money (ATM) volatility (as this is the most liquid swaption strike), the slope can be defined as the difference between highest strike ( $+200\text{bps}$ ) and lowest strike ( $-200\text{bps}$ ) volatility, while the curvature can be defined as the ATM volatility relative to an average of highest strike and lowest strike volatilities:

$$\text{Empirical Level Proxy} = \sigma_{\text{ATM}}$$

$$\text{Empirical Skew Proxy} = \sigma_{\text{ATM}+200\text{bps}} - \sigma_{\text{ATM}-200\text{bps}}$$

$$\text{Empirical Smile Proxy} = -2 \times \sigma_{\text{ATM}} + \sigma_{\text{ATM}-200\text{bps}} + \sigma_{\text{ATM}+200\text{bps}} \text{ Black Volatility}$$

To provide a visual illustration of our empirical analysis, we present our estimates for each of the implied volatility empirical proxies in Figure 7. We use 3%-shifted implied lognormal volatility quotes in this figure. The 3 figures on the left column plot empirical level, skew, and smile against forward swap rates, while the 3 figures on the right column plot the time series of the empirical measures. From the left figures, it should be obvious that the dependence of empirical level, skew (slope), and smile (curvature) of the implied volatility surface are all consistent with earlier observations (see Figure 2, 3, and 4) computed based on rate movements. The time series plots on the right also show that the onset of negative rate regime leads to higher volatility level and smile, while skew becomes negative.

## 4 Model

### 4.1 Volatility Backbone

Let  $F_t$  denote the forward swap rate for a given expiry and tenor at time  $t$ . Under a model following normal distribution, the volatility of interest rate movements over time is independent of the interest rate

level. This can be expressed as the following stochastic differential equation:

$$dF_t = \sigma_n dW_t \quad \Rightarrow \quad F_t = F_0 + \sigma_n W_t,$$

where  $\sigma_n$  is the normal volatility of the swap rate, and  $W_t$  is a standard Brownian motion with the distribution  $W_t \sim N(0, t)$ . In words,  $F_t$  behaves like a random walk. In contrast, under a model following lognormal distribution, the volatility of interest rate movements over time is proportional to the interest rate level, such that high rates are associated with high volatilities, and vice versa. This can be expressed in the following stochastic differential equation:

$$dF_t = \sigma_{ln} F_t dW_t \quad \Rightarrow \quad F_t = F_0 e^{-\frac{\sigma_{ln}^2 t}{2} + \sigma_{ln} W_t}.$$

where  $\sigma_{ln}$  is the lognormal volatility of the swap rate. In words, under lognormal dynamics, it is the log rates that behave like a random walk. Whether forward rates follow a normal dynamic, a lognormal dynamic, or a mixture of normal and lognormal dynamics, has important implication on the risk management of swaption portfolio.

Here we present an intuitive explanation of the implication of choosing the right volatility backbone on risk management of swaption portfolio. Consider the following processes:

$$\begin{cases} \text{Normal model : } dF_t = \sigma_n dW_t \\ \text{Lognormal model : } dF_t = \sigma_{ln} F_t dW_t \\ \text{CEV model : } dF_t = \sigma_{cev} F^\beta dW_t \end{cases}$$

Suppose  $\beta = 1$ , market follows a lognormal volatility backbone, and any movement in the forward rates will result in the same implied lognormal volatility. On the other hand, if  $\beta = 0$ , market follows a normal backbone, and any movement in the forward rates will result in identical normal volatility. It should be clear that for normal volatility to remain unchanged when rates move, the implied lognormal volatility will have to decrease when rate moves up, and increase when rate moves down. A model between normal and lognormal will imply that as rates increase, the implied volatility will decrease, but not to the extend suggested by the normal model.

Figure 8 plots a series of implied volatility curves under different forward rates of 2%, 4%, 6%, and 8%. For a given volatility backbone, changes in the forward rate  $F_t$  will result in changes in the at-the-money implied volatility  $\sigma_{ATM}$ . The curve traced out by the this ATM volatility as a function of

the forward rate is referred to as the volatility backbone (solid black line). As we will elaborate later in Section 5, choosing the right backbone plays an important role in guaranteeing the robustness of the hedged portfolio. The top figure plots the case for a lognormal volatility backbone ( $\beta = 1$ ) – it should be obvious that the ATM implied Black volatility is invariant to the interest rate level in this case. However, when the backbone is a mixture of normal and lognormal, the ATM implied volatility will be inversely proportional to the rate level — as rates increase, the implied volatilities decrease. This is the case for the lower figure, which plots the case with ( $\beta = 0.7$ ).

We provide a numerical example to illustrate the importance of choosing the optimal backbone ( $\beta$ ) from a risk management perspective. Suppose the market backbone is given by  $\beta_{mkt} = 0.7$ , and that the implied volatilities in the market is plotted in Figure 9 (upper figure). A swaption portfolio manager uses SABR model with the right backbone ( $\beta = \beta_{mkt}$ ) to calibrate to these quotes, and is able to match observed swaption prices with a high degree of accuracy. Suppose another swaption portfolio manager is using an incorrect backbone of  $\beta = 1$ . This portfolio manager will still be able to calibrate to the market with a close match in prices, as denoted by the dashed red line in the figure. In other words, in terms of daily mark-to-market, whether or not the right backbone ( $\beta$ ) is used, portfolio managers will always be able to match market prices closely as long as they recalibrate the model parameters frequently.

However, the disadvantage of choosing the wrong volatility backbone manifests when the portfolio managers are also using the model for hedging and risk management, and to breakdown daily P&L in terms of sensitivity and market movement. Suppose the swap rate increases from 3% to 3.5%, and that the volatility market remains unchanged. For the portfolio manager using the right backbone value of  $\beta = 0.7$ , no changes in the SABR parameters ( $\alpha$ ,  $\rho$ , and  $\nu$ ) is required to match the swaption prices after the move – the P&L movement can be explained entirely by interest rate delta. On the other hand, the portfolio manager using the incorrect backbone of  $\beta = 1$  will have to recalibrate to the swaption market to obtain a new set of SABR model parameters in order to match the market prices. Consequently, under the wrong backbone, the same amount of P&L movement will now have to be explained by delta, vega, and a combination of skew and smile sensitivity.

This scenario case study is summarized in Figure 9. In the upper plot, the solid lines denote the market implied volatility before and after the rate move under the right backbone. Observe that even if a portfolio manager incorrectly assumes the backbone to be  $\beta = 1$ , recalibrating the SABR model after the rate move will still lead to a good fit to market prices, as denoted by the dashed lines in the upper plot in Figure 9. The disadvantage of risk managing swaption portfolio using an incorrect backbone will only manifest when one takes hedging and P&L explanation into consideration. Consider an out-

of-the-money (OTM) receiver swaption struck at 1.5%, and an out-of-the-money payer payer struck at 4%. As we will develop fully in Section 5, the P&L of a swaption position can be explained via a risk-based framework by attributing total movement to sensitivities (Greeks) to market data and model parameters (rates, implied volatilities, and model parameters). As illustrated in the lower plots of Figure 9, the first column is the total price movement of the swaption position. For a given pricing model, we can “explain” this price movement by decomposing and attributing it to interest rate delta (second column) which measures sensitivity to rates movement, interest rate vega (third column) which measures sensitivity to at-the-money volatility movement, and SABR model parameters sensitivities (fourth and fifth columns) which measure the sensitivities of  $\rho$  and  $\nu$  parameters to the shape of the implied volatility surface. Suppose the swap rate moves up, without other changes in the volatility market, the portfolio manager risk managing these OTM receiver (lower left figure) and payer (lower right figure) swaptions with the right backbone of  $\beta = 0.7$  will be able to explain the P&L of the position entirely by interest rate delta, and no recalibration of the model parameters is necessary (lower figures, “Correct  $\beta$ ” plots). On the other hand, the portfolio manager using the incorrect backbone of  $\beta = 1$  will first need to recalibrate the model parameters to match market quotes, and then explain the same P&L movement via offsetting components in interest rate delta, interest rate vega, and skew sensitivities ( $\rho$  and  $\nu$ ) due to the changes in model parameters (lower figures, “Incorrect  $\beta$ ” plots).

While this is a stylized example, it should be evident that SABR model will always able to match market quotes well by frequent recalibration — the advantage of choosing the right volatility backbone only becomes apparent when we assess the efficiency and performance of the model for risk management and P&L explanation. This calls for a more holistic approach to model calibration by also taking Greeks and P&L explanation into consideration as part of the model assessment framework. In fact, apart from P&L explanation, the Greeks themselves are also sensitive to the choice of volatility backbone, as we will explain in the next section.

## 4.2 Month-end Jumps and Model Sensitivity

We illustrate the sensitivity of swaption Greeks to jumps in SABR model parameters in this section. Figure 10 plots the results of a longitudinal model calibration over a two-year period. The top two figures show the calibrated model parameters for the SABR  $\rho$  and  $\nu$  parameters, which are used to fit the implied volatility skew and smile profiles, respectively, for the  $20y20y$  swaption. The dotted vertical lines highlight each month-end date, which coincides with jumps in the SABR parameters. These jumps

are due to the fact that interest rate trading desks typically recalibrate their model during month-end. In addition to market data, interest rate trading desks also have access to IHS Markit Totem consensus market prices, which is based on major active market participants in OTC interest rate derivatives market. This leads to a noticeable change in the model parameters. The middle two figures illustrate the sensitivities of at-the-money swaption Greeks to changes in SABR  $\rho$  and  $\nu$  parameters (namely  $\frac{\partial V}{\partial \rho}$  and  $\frac{\partial V}{\partial \nu}$ , where  $V$  denote the value of a swaption). Note that a sudden change in model parameters will result in a corresponding change in model sensitivity. This has important implication on the risk management of swaption portfolios, as Greeks are commonly used to calculate the value-at-risk (VaR) of interest rate portfolios. Consequently, jumps in the model parameters over month-ends will result in corresponding jumps in VaR, even if the model is able to fit prices well before and after each month-end by recalibration, which is an undesirable characteristic for risk managers. The bottom two figures show the P&L movement of at-the-money swaptions straddle (one payer and one receiver) over the two-year period. Offsetting P&L explanation spikes are observed frequently over month-ends due jumps in SABR model parameters. This is again an undesirable effect, as offsetting P&L explanation over consecutive days makes risk management of swaption portfolio less efficient. The implication of model sensitivity to risk management, along with the methodology used to compute P&L explanation, are further elaborated in Section 5.

Apart from risk management, it is important to note that a sizeable change in model parameters can also lead to drastic movement in certain volatility-sensitive interest rate products which are dependent on the shape of the implied volatility smile. For instance, a Constant Maturity Swap (CMS) is sensitive to the shape of the entire volatility smile, and convexity correction is required to get the exact value. The standard practice in the market is to use the static-replication method to obtain the convexity correction. As a result, jumps in model parameters will also lead to jumps in convexity correction.

### 4.3 Displaced-diffusion Stochastic Volatility Model

As mentioned earlier, prior to the negative interest rate regime, the swaption market's convention is to quote prices in terms of implied volatilities of the Black (1976) lognormal model. This convention has since changed as negative rates are inadmissible under lognormal models. An ad hoc workaround to handle negative rates is to shift the rates and strikes up by a predetermined amount. However, shifting the rates will also cause changes the volatility backbone behavior. Another commonly adopted convention is to use a normal model instead. Since a normal model for rate movement allows for negative rates,

this model is able to provide consistent implied volatility quotes without having to ensure that the shift amount is sufficient to guarantee positive forward rates and strikes.

In this section, we propose a displaced-diffusion stochastic volatility model for swaption pricing. The displaced-diffusion model is also widely known in the industry as the shifted-lognormal model. The key strength of the displaced-diffusion process lies in its ability to accommodate negative interest rates without any further additional adjustment. We derive a closed-form analytical expression for swaption pricing, and show that it can also match market prices with a high degree of accuracy.

Consider the displaced-diffusion forward swap rate process as follows

$$dF_t = \sigma[\beta F_t + (1 - \beta)F_0]dW_t, \quad (1)$$

where  $\sigma$  is the volatility,  $\beta$  is the displaced-diffusion model parameter, and  $W_t$  is a standard Brownian motion with  $W_t \sim N(0, t)$ . For now, let us assume that  $\sigma$  is a deterministic constant. We will generalize this to a stochastic volatility model in the later part of this section. The process can also be written as

$$d\left(F_t + \frac{1-\beta}{\beta}F_0\right) = \sigma\beta\left(F_t + \frac{1-\beta}{\beta}F_0\right)dW_t.$$

Written in this way, it should be clear that with  $\left(F_t + \frac{1-\beta}{\beta}F_0\right)$  modeled as a geometric Brownian process, it is strictly positive. Note that, as long as the  $\beta$  parameter is positive, the forward rate process  $F_t$  is now allowed to take on negative values, since the process is well-defined as long as  $F_t + \frac{1-\beta}{\beta}F_0 > 0$ . When  $F_0 > 0$ , any choice of  $0 < \beta < 1$  will provide a negative value as the lowerbound to the forward rate process. This will allow us to price swaptions with negative strikes when forward swap rates are still positive. On the other hand, if  $F_0 < 0$ , then we can choose  $\beta < 0$ , which corresponds to a super-normal process. In this case, we can price swaptions with negative strikes and forward swap rates.

The characteristics of the implied volatility profile and its dependence on the  $\beta$  parameter in the displaced-diffusion model can be intuitively understood by referring to Equation (1), where the evolution of the swap rate can be interpreted as being driven by a weighted average between a lognormal process ( $F_t$ ) and a normal process ( $F_0$ ).

The  $\beta$  parameter in the displaced-diffusion model will allow us to fit the implied volatility skew. A stochastic volatility model is required to calibrate to the smile. To this end, we propose a displaced-

diffusion stochastic volatility model (DDSV) with the following dynamics

$$\begin{cases} dF_t = \sigma_t [\beta(F_t + \theta) + (1 - \beta)F_0] dW_t \\ dV_t = \nu V_t dZ_t \end{cases} \quad (2)$$

where  $W_t$  and  $Z_t$  are independent Brownian motions ( $W_t \perp Z_t$ ), and  $\sigma_t = \sqrt{V_t}$ . We define the mean integrated variance as

$$\bar{V} = \frac{1}{T} \int_0^T V_t dt. \quad (3)$$

Conditional on this mean integrated variance  $\bar{V}$ , we have the distribution

$$\log \left[ \frac{\beta(F_T + \theta) + (1 - \beta)F_0}{F_0 + \beta\theta} \right] \sim N \left( -\frac{\beta^2 \bar{V} T}{2}, \bar{V} T \right).$$

Under the independence assumption, a closed-form valuation formula can be obtained for the DDSV model as:

$$\begin{aligned} P(0) &= A(0) \int_0^\infty DD(F_0, K, \bar{V}, T, \beta) \psi(\bar{V}) d\bar{V} \\ &= A(0) DD(F_0, K, \bar{V}, T, \beta) + \frac{A(0)}{2} \frac{\partial^2 DD(F_0, K, \bar{V}, T, \beta)}{\partial \bar{V}^2} (\mathbb{E}[\bar{V}^2] - \mathbb{E}[\bar{V}]^2) \\ &\quad + \frac{A(0)}{6} \frac{\partial^3 DD(F_0, K, \bar{V}, T, \beta)}{\partial \bar{V}^3} (\mathbb{E}[\bar{V}^3] - 3\mathbb{E}[\bar{V}](\mathbb{E}[\bar{V}^2] - \mathbb{E}[\bar{V}]^2) - \mathbb{E}[\bar{V}]^3) + \dots \end{aligned} \quad (4)$$

where  $A(0) = \sum_{i=1}^N \Delta_{i-1} D(0, T_i)$  is the swap annuity,  $N$  is the total number of swap cashflows,  $\Delta_{i-1}$  is the day count fraction for the period  $[T_{i-1}, T_i]$ , and  $D(0, T_i)$  is a discount factor discounting cashflow from  $T_i$  to 0, and

$$DD(F_0, K, \bar{V}, T, \beta) = F'_0 \Phi \left( \frac{\log \frac{F'_0}{K'} + \frac{\bar{V}' T}{2}}{\sqrt{\bar{V}' T}} \right) - K' \Phi \left( \frac{\log \frac{F'_0}{K'} - \frac{\bar{V}' T}{2}}{\sqrt{\bar{V}' T}} \right) \quad (5)$$

with

$$K' = K + \frac{1 - \beta}{\beta} F_0 + \theta, \quad F'_0 = \frac{F_0}{\beta} + \theta, \quad \bar{V}' = \sqrt{\beta} \bar{V}.$$

The full derivation of this formula is presented in the Appendix section.

Figure 11 provides a comparison of SABR model and the DDSV model formulated in this paper.

It is evident that both models are able to match observed swaption market quotes closely. For the sake of comparison, two dates are shown in this figure: the left figure shows that during positive interest rate regime, both modes fit the market implied lognormal volatility quotes well. However, the right figure shows that as we enter negative interest rate regime, DDSV can still fit the market well without any adjustment, while SABR model is no longer able to calibrate due to negative rates and strikes. As mentioned earlier, practitioners get around this issue by shifting all rates and strikes up by 3% before calibrating the SABR model. The ability to handle negative rates without any ad hoc adjustment is a key advantage of using displaced-diffusion dynamic to model interest rate movement.

Figure 12 plots the volatility backbones of the DDSV model. The upper figure plots implied volatilities with a lognormal volatility backbone with different forward swap rates, while the lower figure plots implied volatilities with a volatility backbone between normal and lognormal with different forward swap rates.

## 5 Model Selection for Optimal Risk Management

So far, we have shown that both SABR and DDSV models are able to reproduce market prices of calibration instruments. On top of that, we have also demonstrated that DDSV model is able to handle negative rates and strikes without any additional “fudge” factor. Next, we will turn our attention to address the rest of the criteria that constitute an optimal model for pricing and hedging — the robustness of calibration and the economy of P&L explanation. This section provides an exposition on the hedging performance of the pricing models in the risk management of swaption portfolio. First, we describe how common measures of sensitivity to market movement (Greeks) are quantified for a given pricing model, and how the daily P&L can be expressed in a risk-based P&L explanation framework.

SABR model provides a closed-form expression for the Black volatility as a function of market and model parameters, i.e.  $\sigma_{\text{SABR}}(\alpha(\sigma_{\text{ATM}}), F, K, \beta, \rho, \nu, T)$ . At-the-money swaptions are very liquid, and must be repriced exactly. It is therefore common among practitioners for the  $\alpha$  parameter to be fitted on-the-fly via a root solver to match the ATM volatility, rather than merely assigning more weights to the ATM swaption in the calibration process. Here,  $\sigma_{\text{ATM}}$  is the at-the-money volatility, marked according to a specific backbone ( $\beta$  parameter). The value of a swaption is valued as

$$V(F_0, K, \sigma_{\text{SABR}}, T) = A(0) \left[ F_0 \Phi \left( \frac{\log \frac{F_0}{K} + \frac{\sigma_{\text{SABR}}^2 T}{2}}{\sigma_{\text{SABR}} \sqrt{T}} \right) - K \Phi \left( \frac{\log \frac{F_0}{K} + \frac{\sigma_{\text{SABR}}^2 T}{2}}{\sigma_{\text{SABR}} \sqrt{T}} \right) \right]$$

As explained in previous sections, once calibrated, both SABR and DDSV models are able to fit market prices very well. Hence, from a risk management perspective, the stability of Greeks and the economy of P&L explanation should be included as part of the selection criteria for the optimal model. If the optimal model is chosen, the bulk of the daily P&L movement should be explained by interest rate delta, with vega explaining the actual changes in the volatility market. Further, sensitivities to implied volatility skew and smile are expected to have a smaller contribution in P&L explanation, as they should only change when the shape of the market's implied volatility surface changes. The sensitivities of the SABR swaption prices are given by

$$\begin{aligned} \text{IR Delta} &= \Delta = \frac{dV}{dF} = \frac{\partial V}{\partial F} + \frac{\partial V}{\partial \sigma_{\text{SABR}}} \cdot \frac{\partial \sigma_{\text{SABR}}}{\partial F} \\ \text{IR Vega} &= \frac{dV}{\sigma_{\text{ATM}}} = \frac{\partial V}{\partial \sigma_{\text{SABR}}} \cdot \frac{\partial \sigma_{\text{SABR}}}{\partial \alpha} \cdot \frac{\partial \alpha}{\partial \sigma_{\text{ATM}}} \\ \text{IR Skew Sensitivity} &= \frac{dV}{d\rho} = \frac{\partial V}{\partial \sigma_{\text{SABR}}} \cdot \frac{\partial \sigma_{\text{SABR}}}{\partial \rho} \\ \text{IR Smile Sensitivity} &= \frac{dV}{d\nu} = \frac{\partial V}{\partial \sigma_{\text{SABR}}} \cdot \frac{\partial \sigma_{\text{SABR}}}{\partial \nu} \end{aligned}$$

Moving from one day ( $t - 1$ ) to the next ( $t$ ), suppose the SABR model parameters ( $\alpha$ ,  $\rho$ , and  $\nu$ ) are calibrated on both days, the P&L of a swaption position over the period  $[t - 1, t]$  can be explained as

$$\begin{aligned} \text{SABR P&L Explanation} &= \frac{dV}{dF} \times (F_t - F_{t-1}) + \frac{dV}{d\sigma_{\text{ATM}}} \times (\sigma_{\text{ATM},t} - \sigma_{\text{ATM},t-1}) \\ &\quad + \frac{dV}{d\rho} \times (\rho_t - \rho_{t-1}) + \frac{dV}{d\nu} \times (\nu_t - \nu_{t-1}) \end{aligned} \tag{6}$$

On the other hand, for the DDSV model, given that the pricing formula provides prices directly, the derivatives (sensitivities) can be evaluated directly:

$$\begin{aligned} \text{IR Delta} &= \Delta = \frac{dV}{dF} \\ \text{IR Vega} &= \frac{dV}{d\sigma} \\ \text{IR Skew Sensitivity} &= \frac{dV}{d\beta} \\ \text{IR Smile Sensitivity} &= \frac{dV}{d\nu} \end{aligned}$$

And the daily P&L can be explained as

$$\begin{aligned} \text{DDSV P\&L Explanation} &= \frac{dV}{dF} \times (F_t - F_{t-1}) + \frac{dV}{d\sigma} \times (\sigma_t - \sigma_{t-1}) \\ &\quad + \frac{dV}{d\beta} \times (\beta_t - \beta_{t-1}) + \frac{dV}{d\nu} \times (\nu_t - \nu_{t-1}). \end{aligned} \quad (7)$$

The actual P&L, which can be readily calculated as the price difference between the two days, is given by

$$V_t = V_{t-1} + \text{P\&L Explanation}_t + \epsilon_t,$$

where  $\epsilon_t$  is the residual difference that cannot be captured by the P&L explanation framework proposed above, which is expected to be negligible, as long as the pricing model is recalibrated and can accurately price the swaption over the period  $[t-1, t]$ . Since the actual P&L is simply given by  $V_t - V_{t-1}$ , we can readily obtain the percentage of explained P&L:

$$\text{Explained P\&L}_t(\%) = \frac{\text{P\&L Explanation}_t}{\text{Actual P\&L}_t}.$$

This P&L performance metric is commonly used by practitioners to gauge the explanatory power of a pricing model. In both Equations (6) and (7), the explanation is not expected to match exactly the actual P&L. The residual ( $\epsilon_t$ ) is typically quantified as “unexplained” P&L, though an efficient model for risk management should be able to provide an accurate P&L breakdown with negligible “unexplained” component.

Figure 13 provides a comparison of hedging performance across different swaption pricing models by running the daily P&L explanation framework over a 1-year period (Oct 2016 through to Sep 2017). We have selected this period, which falls under the negative interest rate regime, to demonstrate the advantage of the DDSV model in handling negative strikes without ad hoc adjustment. The same analysis can be applied to other periods to obtain comparable results. We assume we hold a portfolio of one swaption each across the strike chain (OTM receivers, ATM straddle, OTM payers). On each date, we calibrate the SABR and DDSV models to the market and ensure convergence of the calibration process. Then, we compute the P&L explanation based on our proposed framework. For the sake of comparison, for SABR we use a 3%-shifted model, and we vary the  $\beta$  parameter from 0 (normal model) to 1 (lognormal model) with a spacing of 0.1. For DDSV model, we use a  $\beta$  parameter calibrated longitudinally for optimal hedging performance. The top figure shows the contributions of each risk to

the overall P&L breakdown, calculated as the absolute sum of each category, defined as follows:

$$\begin{aligned}
 \text{Abs. Delta P\&L} &= \sum_{t=1}^n \left| \frac{\partial V}{\partial F} \cdot (F_t - F_{t-1}) \right| \\
 \text{Abs. Vega P\&L} &= \sum_{t=1}^n \left| \frac{\partial V}{\partial \sigma} \cdot (\sigma_{\text{ATM},t} - \sigma_{\text{ATM},t-1}) \right| \\
 \text{Abs. Skew P\&L} &= \sum_{t=1}^n \left| \frac{\partial V}{\partial \rho} \cdot (\gamma_t - \gamma_{t-1}) \right| \\
 \text{Abs. Smile P\&L} &= \sum_{t=1}^n \left| \frac{\partial V}{\partial \nu} \cdot (\nu_t - \nu_{t-1}) \right|
 \end{aligned} \tag{8}$$

where  $\gamma$  is  $\rho$  for SABR model and  $\beta$  for DDSV model. We take the absolute value to provide a measure of the economy of P&L explanation – the smaller the sum, the better the model. We argue that for a given amount of P&L movement, the optimal model should be able to explain the P&L movement with the smallest amount of offsetting components. As we have demonstrated in Figure 9 in the previous section, a sub-optimal model with a wrong backbone choice will lead to offsetting risk-based P&L explanation, in particular for IR Delta and IR Vega sensitivities. Although our PCA analysis has revealed that there are some degree of overlap between skew and smile, our assumption is that when aggregated over a period of time, the effect of IR Delta and IR Vega dominates. From the upper plot of Figure 13, it is also evident that with the right choice of  $\beta$ , both SABR and DDSV models are able to yield minimal hedging error and achieve economy of P&L explanation.

Based on the empirical observation that IR Delta risk dominates market movement when aggregated over time—while IR Vega, Skew, and Smile are generally secondary risk components—we propose that a stylized way to select the optimal model could be based on the “concentration” of P&L explanation. The main rationale behind using “concentration” as the key metric to measure hedging performance is that the optimal model should generate the least degree of overlap across different risk components, thus reducing the “fragmentation” effect, and improving hedging efficiency. We point out that this is based on the assumption that over time, one primary source of risk would dominate P&L explanation, which is what our empirical analyses have revealed. To this end, measuring “concentration” will lead us to select the most economical model in terms of P&L explanation.

In order to provide a metric to quantify the “concentration” (or “fragmentation”) of the hedging performance of the swaption pricing model in terms of P&L explanation, we borrow the concept of the Herfindahl-Hirschman index from the industrial organization literature. Originally designed as a measure commonly used to measure market concentration, this metric has since been adapted in other

fields for similar purposes. For instance, Madhavan (2012) uses a volume Herfindahl-Hirschman index definition to measure market fragmentation across different US exchanges. Here, we define the hedging performance Herfindahl-Hirschman index as a measure of concentration in P&L breakdown for a given daily P&L movement:

$$H_t = \left( \frac{\left| \frac{\partial V}{\partial F} \cdot (F_t - F_{t-1}) \right|}{\text{Total Abs P&L}_t} \right)^2 + \left( \frac{\left| \frac{\partial V}{\partial \sigma} \cdot (\sigma_{\text{ATM},t} - \sigma_{\text{ATM},t-1}) \right|}{\text{Total Abs P&L}_t} \right)^2 \\ + \left( \frac{\left| \frac{\partial V}{\partial \rho} \cdot (\rho_t - \rho_{t-1}) \right|}{\text{Total Abs P&L}_t} \right)^2 + \left( \frac{\left| \frac{\partial V}{\partial \nu} \cdot (\nu_t - \nu_{t-1}) \right|}{\text{Total Abs P&L}_t} \right)^2$$

where

$$\text{Total Abs P&L}_t = \left| \frac{\partial V}{\partial F} \cdot (F_t - F_{t-1}) \right| + \left| \frac{\partial V}{\partial \sigma} \cdot (\sigma_{\text{ATM},t} - \sigma_{\text{ATM},t-1}) \right| \\ + \left| \frac{\partial V}{\partial \rho} \cdot (\rho_t - \rho_{t-1}) \right| + \left| \frac{\partial V}{\partial \nu} \cdot (\nu_t - \nu_{t-1}) \right|$$

Note that unlike common definition, in the context of P&L explanation it is necessary to take the absolute value as P&L explanation could be either positive or negative. The Herfindahl-Hirschman index in our definition ranges from 0 to 1, with higher figures indicating higher concentration (less fragmentation) in P&L explanation, which is a more desirable characteristics. The lower plot of Figure 13 compares the Herfindahl-Hirschman index across different swaption pricing models. Again, we use a 3% shifted SABR model to handle negative rate regime, while no further adjustment is necessary for the DDSV model. Given the right choice of  $\beta$ , our calculations reveal that both SABR and DDSV models are able to provide optimal hedging performance with highest amount of concentration in P&L breakdown.

We point out that the rationale behind using Herfindahl-Hirschman index to measure hedging performance is based on the assumption that when aggregated over a period of time, swap rate movements (IR Delta) should be able to explain a large part of the swaption price P&L, followed by ATM volatility movements (IR Vega). Changes in the skew and smile profile of the implied volatility curve should, on average, contribute a smaller part to the overall P&L explanation, since movements in the implied volatility skew and smile profiles are comparably more stable than the swap rate movements.

However, there are two main limitations practitioners need to be aware of when using this approach. Firstly, this metric needs to be aggregated over a historical period. If investors are looking to measure the hedging performance on a single day, this metric could potentially lead to a certain amount of bias on days when IR Vega, Skew or Smile contributes significantly to P&L explanation due to extreme

movement in the volatility market. Secondly, while the dominance of IR Delta risk is established in the swaption market, further empirical analysis is required when practitioners wish to apply the same framework to other derivative markets, where IR Vega, Skew and Smile could potentially play a more significant role. Additional research is necessary to establish whether the same metric can be applied widely across different derivative markets and instruments types.

To provide further information on the historical evolution of hedging performances over time, Figure 14 plots the Explained P&L (in percentages) over the same historical period (Oct 2016 through to Sep 2017). In order to have a basis for comparison, we present the DDSV model along with a shifted SABR model with a  $\beta$  parameter of 1, which in our analysis is a sub-optimal model due to the inappropriate choice of volatility backbone. The Explained P&L plot supports our argument by showing that a frequently recalibrated model can generally match market well, leading to, on average, close to 100% explained P&L in both models. Consequently, it is difficult to tell whether the optimal model has been selected by looking at explained P&L alone. This observation lends support to the risk-based model selection approach—we need to measure the concentration of hedging performance in order to distinguish the hedging performance of different models. In other words, the optimal model should be the one that enables us to explain the same amount of P&L movement by a smaller set of risks and sensitivities.

Our results reported in this section have important and insightful implication to all interest rate and fixed-income portfolio managers with volatility exposure. Standard practice in the market is to heuristically select a backbone parameter, and to calibrate the rest of the model parameters to match observed market prices. Our research shows the advantage of taking a holistic approach to the calibration process for optimal model selection. In addition to matching observed market prices, the stability and robustness of model parameters, and the economy of the explanatory power of daily P&L movement, are part and parcel of factors that determine an optimal pricing and hedging model.

## 6 Conclusions

The interest rate markets use swaptions as the main interest rate volatility instrument. In addition to hedging fixed income portfolio, traders also use swaptions to gain interest rate risk exposure, or to structure more exotics products such as CMS payoffs, Bermudan swaptions, and callable interest rate exotics. Therefore, efficient risk management of swaptions portfolio impacts the whole spectrum of interest rate volatility products.

The primary objective of this paper is to formulate a risk management framework with P&L explan-

ation capability for optimal model selection. As a case study, we demonstrate the application of our framework using the recent transition of interest rate regime in the Eurozone from moderate to negative, and the behavior of volatility of daily rate movement. We perform empirical analyses to explore the relationship between interest rate level with the standard deviation, skewness, and kurtosis of daily rate changes. Lower rate levels are associated with higher standard deviation and kurtosis of daily rate changes, but more negative skewness. These empirical observations are fully consistent with standard swaption trading desk notion of risk managing swaption portfolio using a SABR  $\beta$  parameter closer to 0 when rates are low, while using a  $\beta$  parameter closer to 1 when rates are moderate to high. We apply Principal Component Analysis (PCA) to the daily changes in implied volatility surface. Our results show that implied volatility level (first PC), slope (second PC), and curvature (third PC) collectively account for more than 99.5% of the movement in implied volatility surface. This is a strong indication that market's practice of using SABR model to price and hedge swaption portfolio is well-informed, as apart from the backbone parameter ( $\beta$ ), the SABR model's  $\alpha$ ,  $\rho$ , and  $\nu$  parameters correspond to the level, slope, and curvature of the implied volatility surface, respectively.

We also demonstrate that selecting an optimal backbone is vital to ensure the stability and robustness of the calibrated model parameters. This is no trivial task, given that SABR model is able to fit swaption market prices extremely well. To assess calibration stability, we investigate the sensitivity in Greeks and P&L explanation for non-optimal choice of backbone, and show that this can lead to sizeable jumps when market moves. The challenge of choosing the optimal backbone is further confounded by the negative interest rate regime in the Eurozone, as it becomes necessary to shift the rate levels (and strikes) to price swaptions using SABR model, since both the  $\beta$  parameter and the shift amount impact the backbone behavior of the model.

We formulate a closed-form analytical swaption pricing model capable of handling negative rates and strikes in a consistent manner is essential for swaption portfolio managers. Note that any alternative swaption pricing model must retain the analytical tractability and computational speed of the SABR model to be feasible for daily portfolio risk management purposes. In this paper, we derive a closed-form pricing formula based on displaced-diffusion stochastic volatility model. The displaced-diffusion dynamic is able to handle negative rates and strikes. We show that the model is able to fit the market quotes as well as SABR model, and is able to calibrate well in the negative interest rate regime when forward swap rates or strikes are negative without any further ad hoc adjustment.

Finally, building on the insights of Zhang and Fabozzi (2016), we set out a swaption portfolio risk management framework that accounts for variation in forward rates, implied volatilities, as well as the

shape of the implied volatility curve (skew and smile). Any adequate pricing model should at least to be able to fit to market quotes well, as long as the model parameters are calibrated frequently. When the right backbone is chosen, the bulk of the daily P&L should be explained by interest rate delta, followed by interest rate vega. Changes in skew and smile are expected to be slowly varying compared to rates movement. Nevertheless, if a sub-optimal backbone is chosen, daily calibration of the model parameters will still ensure that we fit the market well, and are able to capture the daily P&L movement. However, the P&L explanation will have offsetting contribution from Greeks and model sensitivities. We demonstrate how one can select the optimal model via a holistic approach, by taking the robustness of model parameters and the economy of P&L explanation into consideration during the calibration process. Given the right choice of volatility backbone, we show that it is feasible for SABR and DDSV models to obtain optimal P&L breakdown performance. Our results provide important insights for swaption portfolio managers in choosing the optimal model for risk management.

## References

- Andersen, L. B. G. and Piterbarg, V. V. (2010), *Interest Rate Modeling. Volume III: Products and Risk Management*. Atlantic Financial Press.
- Anthonov, A., Konikov, M. and Spector, M. (Sept. 2015a), ‘The free boundary SABR: natural extension to negative rates’, *Journal of Risk*, pp. 2–7.
- Anthonov, A., Konikov, M. and Spector, M. (Aug. 2015b), ‘Mixing SABR models for negative rates’, *Working Paper*, [Online] Available at SSRN: <https://ssrn.com/abstract=2653682>.
- Black, F. (1976), ‘The pricing of commodity contracts’, *Journal of Financial Economics* **3** (1-2), pp. 167–179.
- Black, F. (1995), ‘Interest rates as options’, *Journal of Finance* **50** (5), pp. 1371–1376.
- Brigo, D. and Mercurio, F. (2006), *Interest rate models – theory and practice: with smile, inflation and credit*, New York: Springer.
- Chen, R.-R., Hsieh, P.-L. and Huang, J. (2018), ‘It is time to shift log-normal’, *Journal of Derivatives* **25** (3), pp. 89–103.
- Cox, J. C. (1996), ‘The constant elasticity of variance option pricing model’, *Journal of Portfolio Management* **23** (5), pp. 15–17.
- Cox, J. C. and Ross, S. A. (1976), ‘The valuation of options for alternative stochastic processes’, *Journal of Financial Economics* **3**, pp. 145–166.
- Deguillaume, N., Rebonato, R. and Pogudin, A. (2013), ‘The nature of the dependence of the magnitude of rate moves on the rates levels: a universal relationship’, *Quantitative Finance* **13** (3), pp. 351–367.
- Duyvesteyn, J. and de Zwart, G. (2015), ‘Riding the swaption curve’, *Journal of Banking & Finance* **59**, pp. 57–75.
- Fan, R., Gupta, A. and Ritchken, P. (2007), ‘On pricing and hedging in the swaption market’, *Journal of Derivatives* **15** (1), pp. 9–33.
- Hagan, P., Kumar, D., Lesniewski, A. and Woodward, D. (Sept. 2002), ‘Managing Smile Risk’, *Wilmott*, pp. 84–108.

- Heston, S. L. (1993), ‘A closed-form solution for options with stochastic volatility with applications to bond and currency options’, *Review of Financial Studies* **6**, pp. 327–343.
- Hull, J. and White, A. (1987), ‘The pricing of options on assets with stochastic volatilities’, *Journal of Finance* **42** (2), pp. 281–300.
- Joshi, M. S. and Rebonato, R. (2003), ‘A displaced-diffusion stochastic volatility LIBOR market model: motivation, definition and implementation’, *Quantitative Finance* **3** (6), pp. 458–469.
- Lee, R. and Wang, D. (2012), ‘Displaced lognormal volatility skews: analysis and applications to stochastic volatility simulations’, *Annals of Finance* **8** (2-3), pp. 159–181.
- Levin, A. (2004), ‘Interest rate model selection’, *Journal of Portfolio Management* **30** (2), pp. 74–86.
- Madhavan, A. (2012), ‘Exchange-Traded Funds, Market Structure, and the Flash Crash’, *Financial Analysts Journal* **68** (4), pp. 20–35.
- Marris, D. (1999), ‘Financial option pricing and skewed volatility’, MPhil Thesis, Statistical Laboratory, University of Cambridge.
- Meucci, A. and Loregian, A. (2016), ‘Neither “normal” nor “lognormal”: modeling interest rates across all regimes’, *Financial Analysts Journal* **72** (3), pp. 68–82.
- Rubinstein, M. (1983), ‘Displaced diffusion option pricing’, *Journal of Finance* **38**, pp. 213–217.
- Siegel, L. B. and Sexauer, S. C. (2017), ‘Five mysteries surrounding low and negative interest rates’, *Journal of Derivatives* **43** (3), pp. 77–86.
- Svoboda-Greenwood, S. (2009), ‘Displaced diffusion as an approximation of the constant elasticity of variance’, *Applied Mathematical Finance* **16** (3), pp. 269–286.
- Wu, T. L. (2012), ‘Pricing and hedging the smile with SABR: evidence from the interest rate caps market’, *Journal of Futures Markets* **32** (8), pp. 773–791.
- Yang, Y., Fabozzi, F. J. and Bianchi, M. L. (2015), ‘Stochastic alpha-beta-rho hedging for foreign exchange options: is it worth the effort?’, *Journal of Derivatives* **23** (2), pp. 76–89.
- Zhang, M. and Fabozzi, F. J. (2016), ‘On the estimation of the SABR model’s beta parameter: the role of hedging in determining the beta parameter’, *Journal of Derivatives* **24** (1), pp. 48–57.

# Appendices

## A Derivation of the Displaced-Diffusion Stochastic Volatility (DDSV) Model

The displaced-diffusion stochastic volatility (DDSV) model is defined by the following dynamics:

$$\begin{cases} dF_t = \sigma_t [\beta(F_t + \theta) + (1 - \beta)F_0] dW_t \\ dV_t = \nu V_t dZ_t \end{cases} \quad (\text{A1})$$

where  $W_t$  and  $Z_t$  are independent Brownian motions ( $W_t \perp Z_t$ ), and  $\sigma_t = \sqrt{V_t}$ . Under this formulation, we model the stochastic variance as a lognormal process. Solving the displaced-diffusion process for  $F_t$  in Equation (A1), we obtain

$$F_T = \frac{F_0}{\beta} \exp \left[ -\frac{\beta^2}{2} \int_0^T V_t dt + \beta \int_0^T \sqrt{V_t} dZ_t \right] - \frac{1 - \beta}{\beta} F_0 - \theta,$$

For convenience of representation, we define the mean integrated variance ( $\bar{V}$ ) as

$$\bar{V} = \frac{1}{T} \int_0^T V_t dt. \quad (\text{A2})$$

Conditional on this mean integrated variance  $\bar{V}$ , we have the following distribution for the forward rate process

$$\log \left[ \frac{\beta(F_T + \theta) + (1 - \beta)F_0}{F_0 + \beta\theta} \right] \sim N \left( -\frac{\beta^2 \bar{V} T}{2}, \bar{V} T \right).$$

Let  $f(F_T, \bar{V})$  denote the joint probability density function of the forward swap rate and the mean integrated variance, and let  $P(0)$  denote the value of a payer swaption at time  $t = 0$ , we can value the swaption as follows

$$P(0) = A(0) \int_0^\infty \int_0^\infty (F_T - K)^+ f(F_T, \bar{V}) dF_T d\bar{V},$$

where  $A(0) = \sum_{i=1}^N \Delta_{i-1} D(0, T_i)$  is the swap annuity,  $N$  is the total number of swap cashflows,  $\Delta_{i-1}$  is the day count fraction for the period  $[T_{i-1}, T_i]$ , and  $D(0, T_i)$  is the discount factor discounting cashflow from  $T_i$  to 0. Under the assumptions that the forward rate movements are uncorrelated with the variance process, the joint probability density  $f(F_T, \bar{V})$  can be written as

$$f(F_T, \bar{V}) = \psi(\bar{V}) f(F_T | \bar{V}),$$

where  $\psi$  denote the probability density function of the mean integrated variance  $\bar{V}$  in Equation (A2). In this case, we have

$$P(0) = A(0) \int_0^\infty \int_0^\infty (F_T - K)^+ f(F_T | \bar{V}) dF_T \psi(\bar{V}) d\bar{V}.$$

Now, the expected value of the sum of the swaption payoffs over all forward rates conditional on a fixed mean integrated variance is equal to the displaced-diffusion formula, which has a closed-form expression

$$\begin{aligned} & \text{Displaced-Diffusion}(F_0, K, \bar{V}, T, \beta) \\ &= \frac{1}{\sqrt{2\pi}} \int_{-\infty}^\infty \left( \left( \frac{F_0}{\beta} + \theta \right) \exp \left[ -\frac{\beta^2 \bar{V} T}{2} + \beta \sqrt{\bar{V} T} x \right] - \frac{1-\beta}{\beta} F_0 - K - \theta \right)^+ e^{-\frac{x^2}{2}} dx \\ &= \frac{1}{\sqrt{2\pi}} \int_{-\infty}^\infty \left( F'_0 e^{-\frac{\bar{V}' T}{2} + \sqrt{\bar{V}' T} x} - K' \right)^+ e^{-\frac{x^2}{2}} dx \\ &= F'_0 \Phi \left( \frac{\log \frac{F'_0}{K'} + \frac{\bar{V}' T}{2}}{\sqrt{\bar{V}' T}} \right) - K' \Phi \left( \frac{\log \frac{F'_0}{K'} - \frac{\bar{V}' T}{2}}{\sqrt{\bar{V}' T}} \right) \end{aligned} \tag{A3}$$

where

$$K' = K + \frac{1-\beta}{\beta} F_0 + \theta, \quad F'_0 = \frac{F_0}{\beta} + \theta, \quad \bar{V}' = \sqrt{\beta} \bar{V},$$

and

$$\Phi(x) = \frac{1}{\sqrt{2\pi}} \int_{-\infty}^x e^{-\frac{u^2}{2}} du$$

is the cumulative distribution function for the standard normal distribution. In other words, since  $\log \left[ \frac{\beta F_T - (1-\beta) F_0}{F_0 + \beta \theta} \right]$  conditional on  $\bar{V}$  is normally distributed with known mean and variance (under the assumption that  $F_t$

and  $V_t$  are uncorrelated), the inner integral becomes the closed-form displaced-diffusion formula. As one can see in Equation A3, the displaced-diffusion payer swaption price can be evaluated using the Black model as a closed-form formula by simply transforming the parameters ( $F'$ ,  $K'$  and  $\bar{V}'$ ). Let  $DD$  denote the displaced-diffusion formula in Equation A3, we can write

$$P(0) = A(0) \int_0^\infty DD(F_0, K, \bar{V}, T, \beta) \psi(\bar{V}) d\bar{V}$$

The DDSV option price is therefore the weighted sum over the displaced-diffusion formula for different integrated variance. This intuitive and elegant result is often referred to as the “mixing” theorem, and is first derived by Hull and White (1987).

Since  $\bar{V}$  is path-dependent, it is difficult to obtain an analytical form of the distribution for  $\bar{V}$ . However, as pointed out by Hull and White (1987), while the distribution of the integrated variance  $\bar{V}$  is unknown, its moments can be readily evaluated. The first three moments are given by:

$$\mathbb{E}[\bar{V}] = V_0, \quad \mathbb{E}[\bar{V}^2] = \frac{2(e^{\nu^2 T} - \nu^2 T - 1)}{\nu^4 T^2} V_0^2, \quad \mathbb{E}[\bar{V}^3] = \frac{e^{3\nu^2 T} - 9e^{\nu^2 T} + 6\nu^2 T + 8}{3\nu^6 T^3} V_0^3.$$

Using Taylor expansion, we expand the DDSV pricing formula around its expected value to obtain

$$\begin{aligned} P(0) &= A(0) \int_0^\infty DD(F_0, K, \bar{V}, T, \beta) \psi(\bar{V}) d\bar{V} \\ &= A(0) DD(F_0, K, \bar{V}, T, \beta) + \frac{A(0)}{2} \frac{\partial^2 DD(F_0, K, \bar{V}, T, \beta)}{\partial \bar{V}^2} (\mathbb{E}[\bar{V}^2] - \mathbb{E}[\bar{V}]^2) \\ &\quad + \frac{A(0)}{6} \frac{\partial^3 DD(F_0, K, \bar{V}, T, \beta)}{\partial \bar{V}^3} (\mathbb{E}[\bar{V}^3] - 3\mathbb{E}[\bar{V}](\mathbb{E}[\bar{V}^2] - \mathbb{E}[\bar{V}]^2) - \mathbb{E}[\bar{V}]^3) + \dots \end{aligned} \tag{A4}$$

For sufficiently small values of  $\nu$  (volatility of volatility), the series converges quickly. Higher accuracy can be attained by adding higher order corrections to the expansion series. Once calibrated to swaption market quotes, Equation (A4) provides an alternative way for us to evaluate swaption prices using closed-form expression. The main advantage of our proposed model over SABR model is that it can incorporate negative rates without any further tweak or adjustment, allowing it to be used consistently in both positive and negative interest rate regimes.

Table I: Summary of Data Set

Expiries	20	1m, 2m, 3m, 6m, 9m, 1y, 18m, 2y, 3y, 4y, 5y, 6y, 7y, 8y, 9y, 10y, 15y, 20y, 25y, 30y
Tenors	15	1y, 2y, 3y, 4y, 5y, 6y, 7y, 8y, 9y, 10y, 15y, 20y, 25y, 30y
Moneyness	15	ATM, $\pm 25bp$ , $\pm 50bp$ , $\pm 75bp$ , $\pm 100bp$ , $\pm 150bp$ , $\pm 200bp$ , $\pm 300bp$

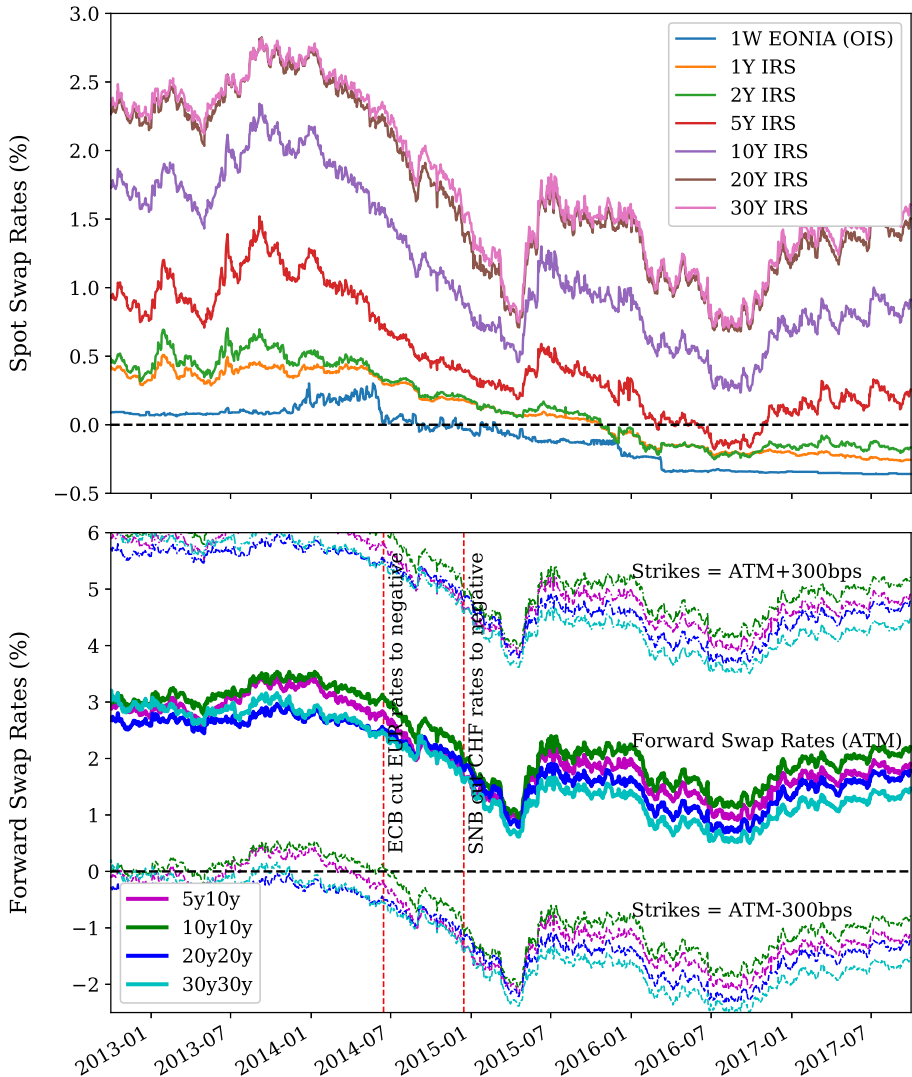
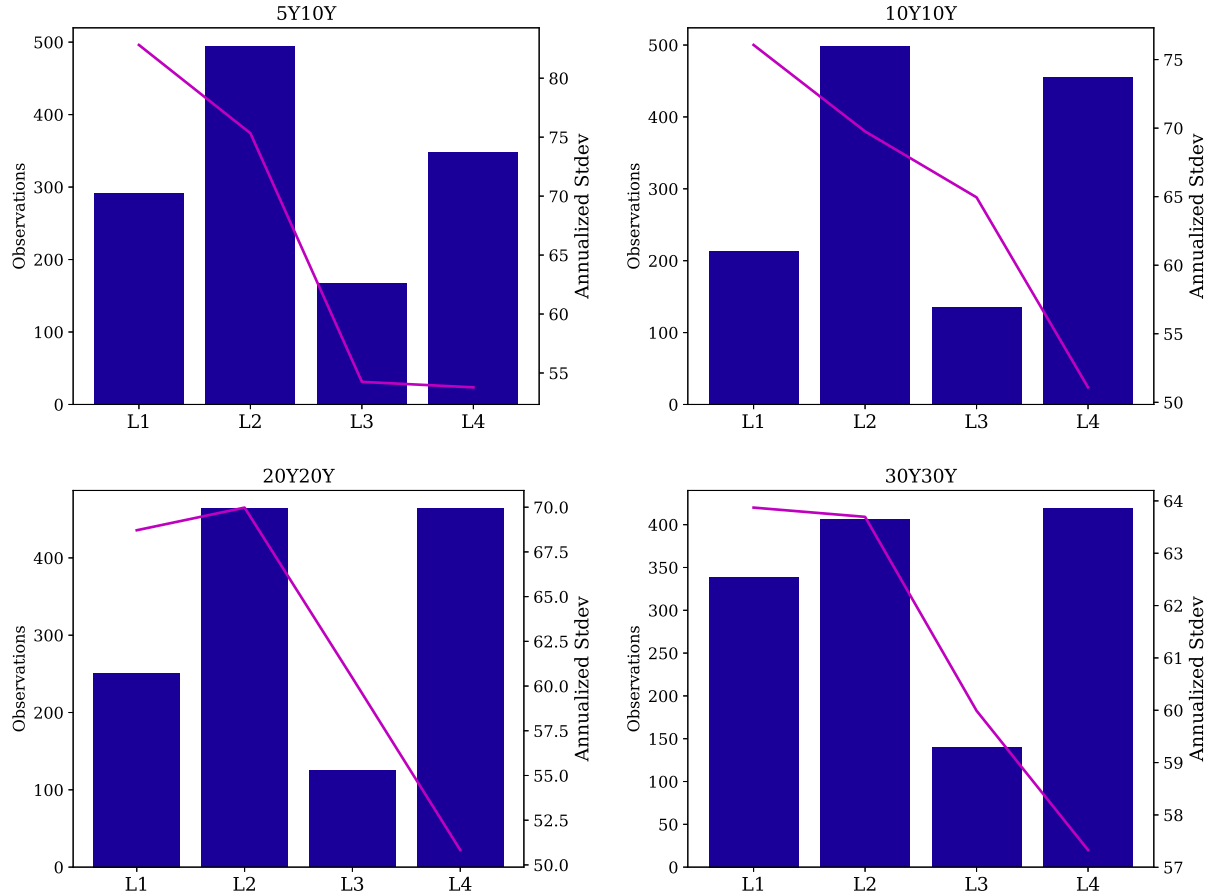
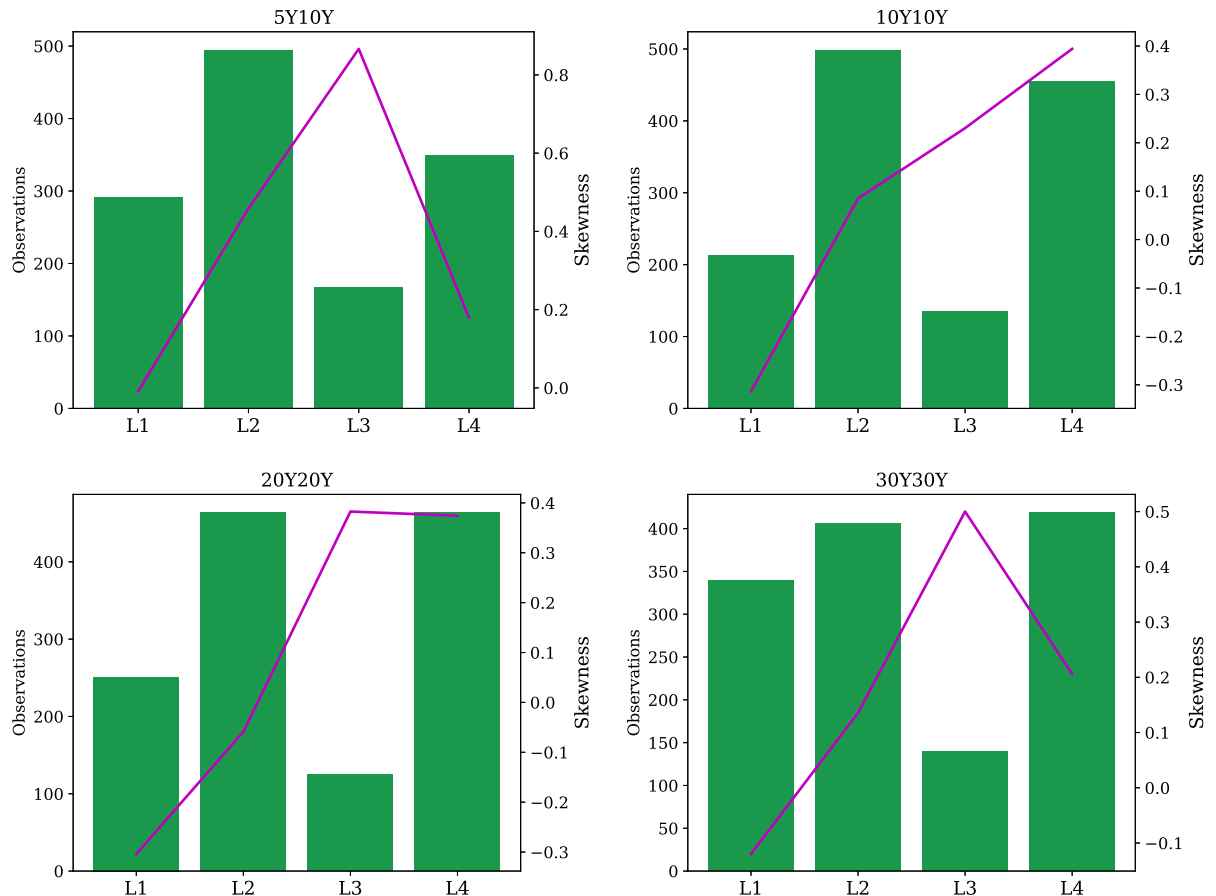


Figure 1: Eurozone swap rates over the 5-year period studied in this paper. The top figure shows the spot starting par swap rates of 1-week EONIA overnight index swap (OIS) and interest rate swaps (IRS) with increasing maturities. The bottom figure shows the forward swap rates (solid lines), which are the relevant parameters used for swaption pricing, along with the strikes at forward swap rates (ATM strike)  $\pm$  300 basis points (dashed lines). ECB cuts EONIA rate to negative in June 2014, but the low strikes swaptions (OTM receivers) already have negative strikes much earlier.



**Figure 2:** Standard deviations of forward swap rate daily changes plotted against the forward swap rate levels, grouped into 4 rate levels. As rates increase, the standard deviations (volatilities) decrease (solid line and right axis). This is consistent with the observed volatility backbone behavior in the swaption market, and in line with standard practice of using a higher  $\beta$  parameter during high rates regime, and lower  $\beta$  parameter during low rates regime. The bar charts (left axis) indicate the number of observations in each group.



**Figure 3:** Skewness of forward swap rate daily changes plotted against the forward swap rate levels. Our empirical results show that as rates increase, the skewness increases (solid line and right axis) from being negative to positive. This statistical behavior is also conforming with the observed volatility backbone in the swaption market, as normal distribution has 0 skewness, while a lognormal distribution exhibits positive skewness. The bar charts (left axis) indicate the number of observation in each group.

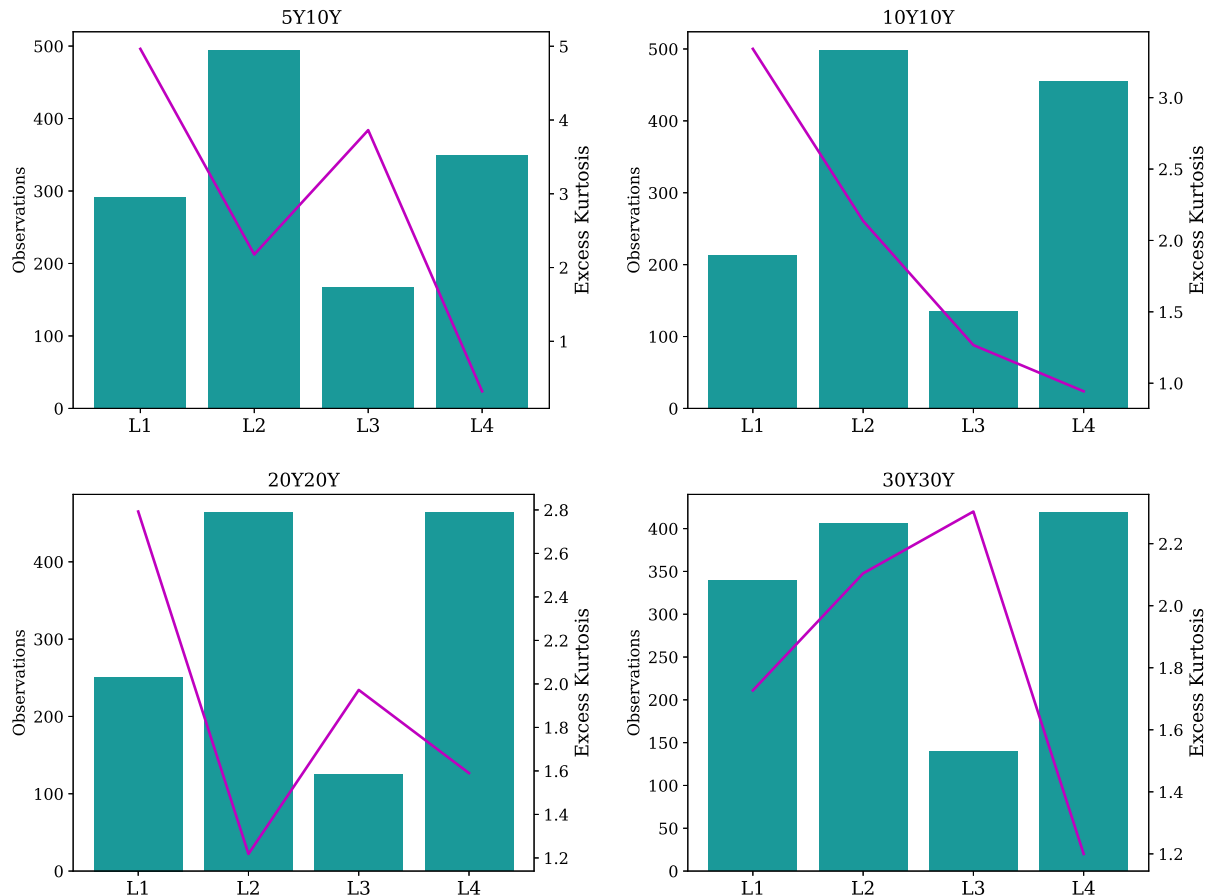


**Figure 4:** Excess kurtosis of forward swap rate daily changes plotted against the forward swap rate level. Our empirical results show that as rates increase, the excess kurtosis decrease (solid line right axis). Note that the excess kurtosis are all positive, implying that the distributions of daily rate changes have heavier tail than normal distribution. The bar charts (left axis) indicate the number of observation in each group.

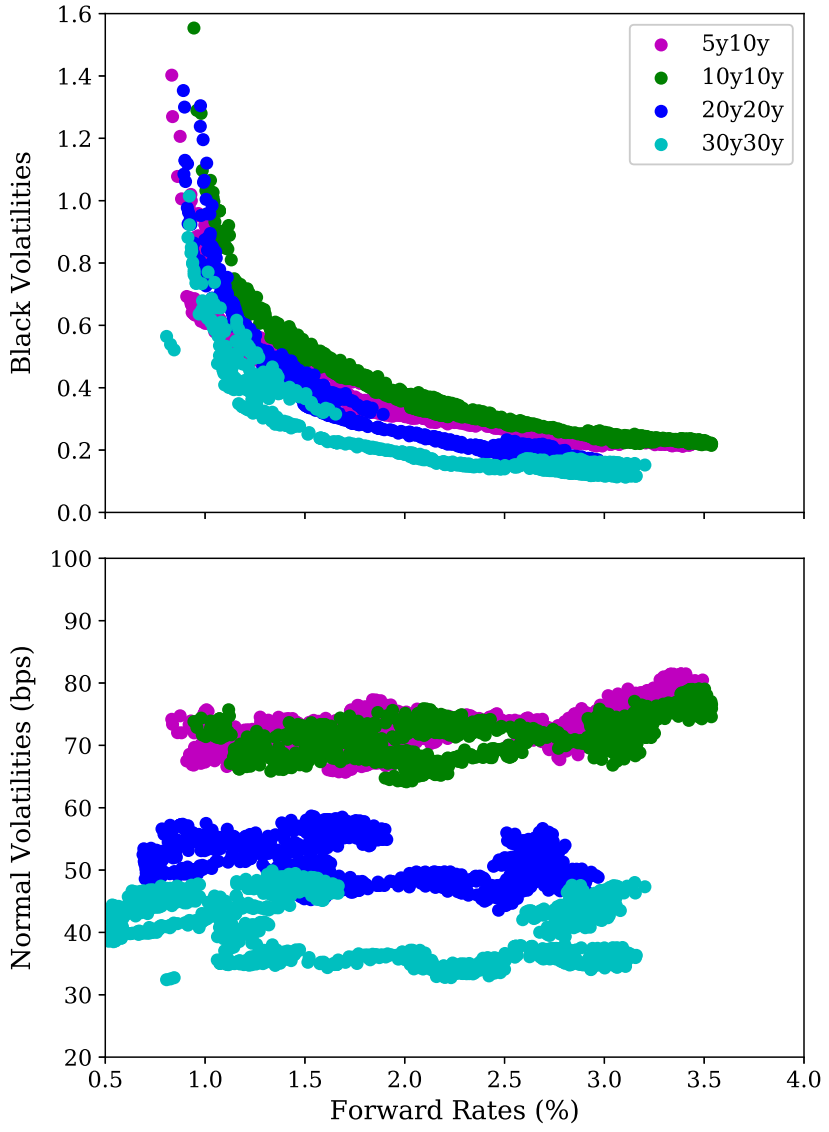


**Figure 5:** Graphical illustration of the volatility backbone behavior in the swaption market. The upper figure plots the Black implied lognormal volatilities against forward swap rates. As is obvious from the graph, lower rates are associated with higher implied lognormal volatilities, while higher rates are associated with lower implied volatilities — this is a clear indication that the volatility backbone is not lognormal. The lower figure plots the implied normal volatilities against forward swap rates. Note that lower rates are associated with a relatively flat implied normal volatilities, while for higher rates the normal volatilities are moderately upward sloping. This indicates that the volatility backbone is between normal and lognormal.

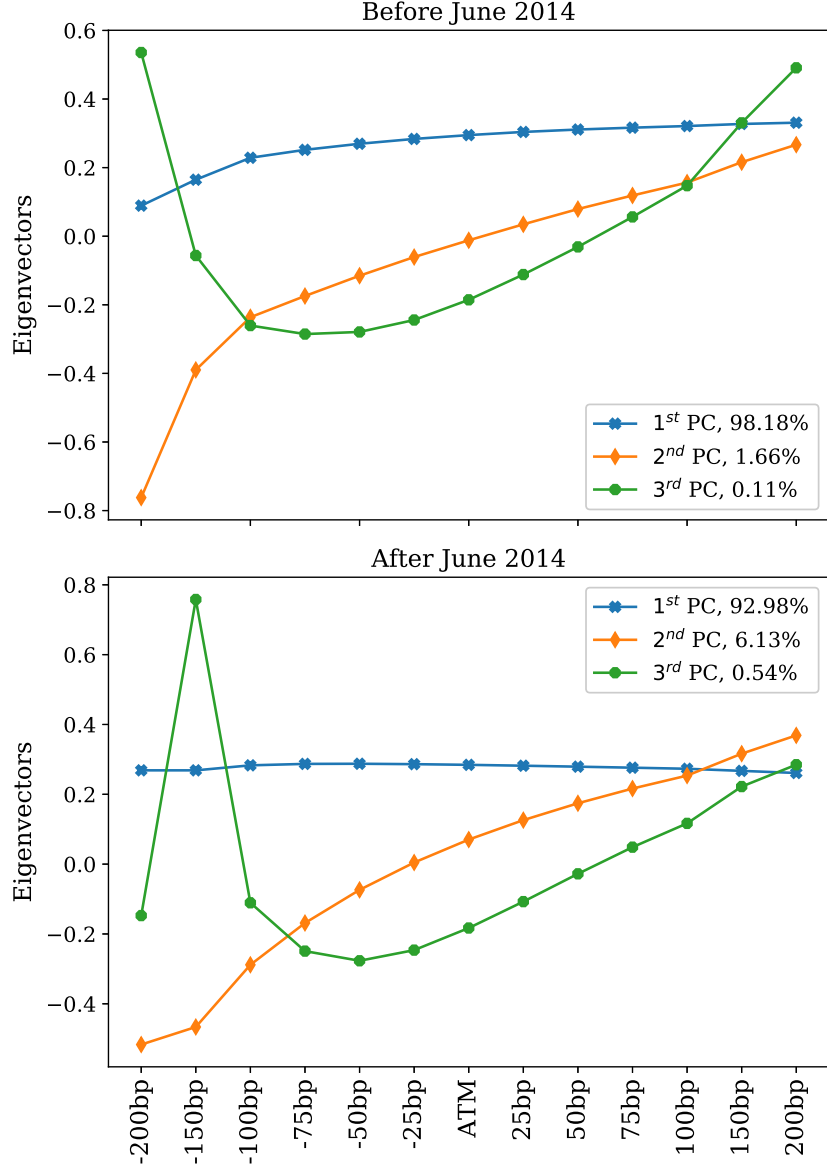


**Figure 6:** Principal components of daily changes in shifted (3%) lognormal implied volatility of 20y20y swaption. We split our data into a “moderate” rate regime (Oct-2012 to Jun-2014) and a “low” rate regime (Jul-2014 to Sep-2017). From the figure, we see that the first three components correspond to the level, slope, and curvature of the implied volatility curves, respectively. On aggregate, the first three components account for more than 99.6% of the shape movements. This is a clear indication that the dynamics of the SABR model has sufficient degree of freedom to capture the shape variation of the implied volatility curves. In the lower figure, an abrupt drop in value is observed on the 3<sup>rd</sup> PC for the  $-200\text{bp}$  strike point, which might be attributed to illiquid data point for very low (negative) strike swaptions during the negative rate regime.

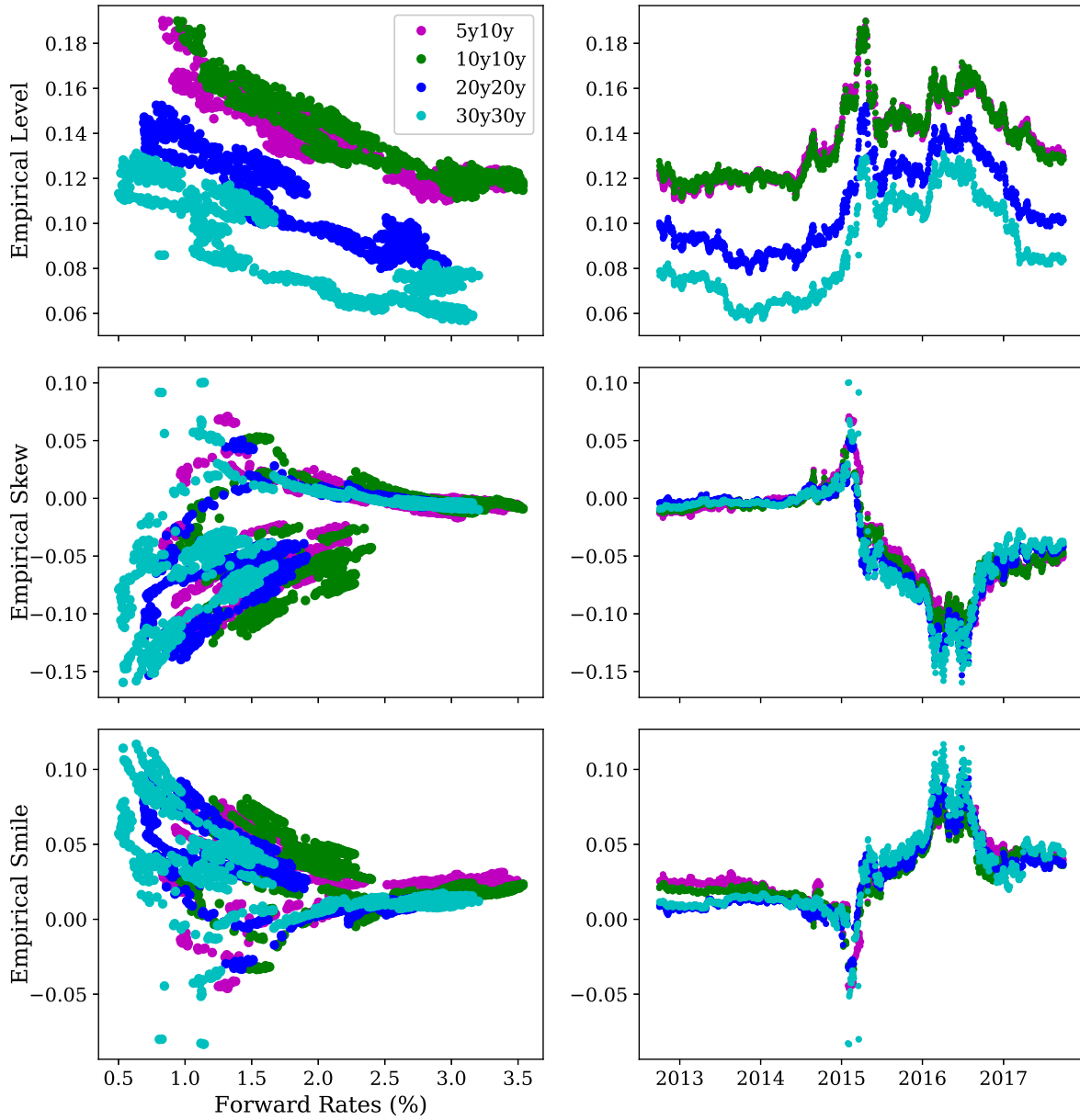


Figure 7: Empirical implied lognormal volatility's level, skew (slope), and smile (curvature) with a 3% shift. The left figures are plotted against forward swap rates, and the right figures are plotted across time. The dependence of empirical level, slope and curvature on rate levels are all consistent with earlier observation. The time series plots (right figures) also show that the onset of negative rate regime leads to higher volatility level and smile, while skew becomes negative.

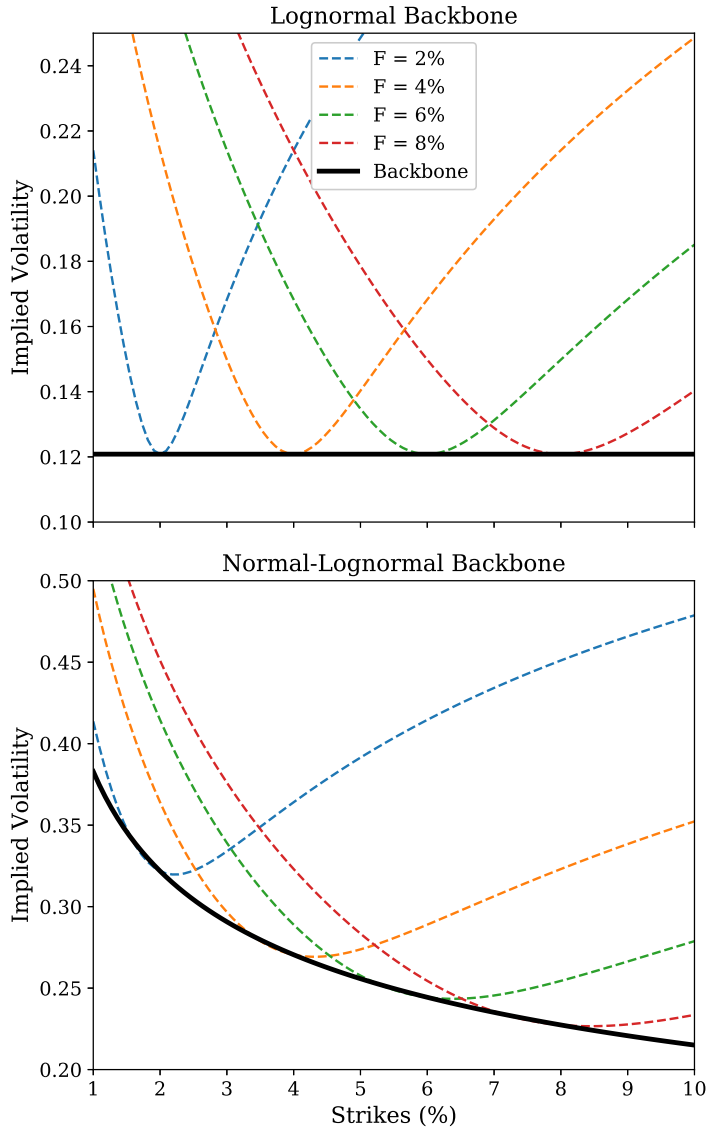
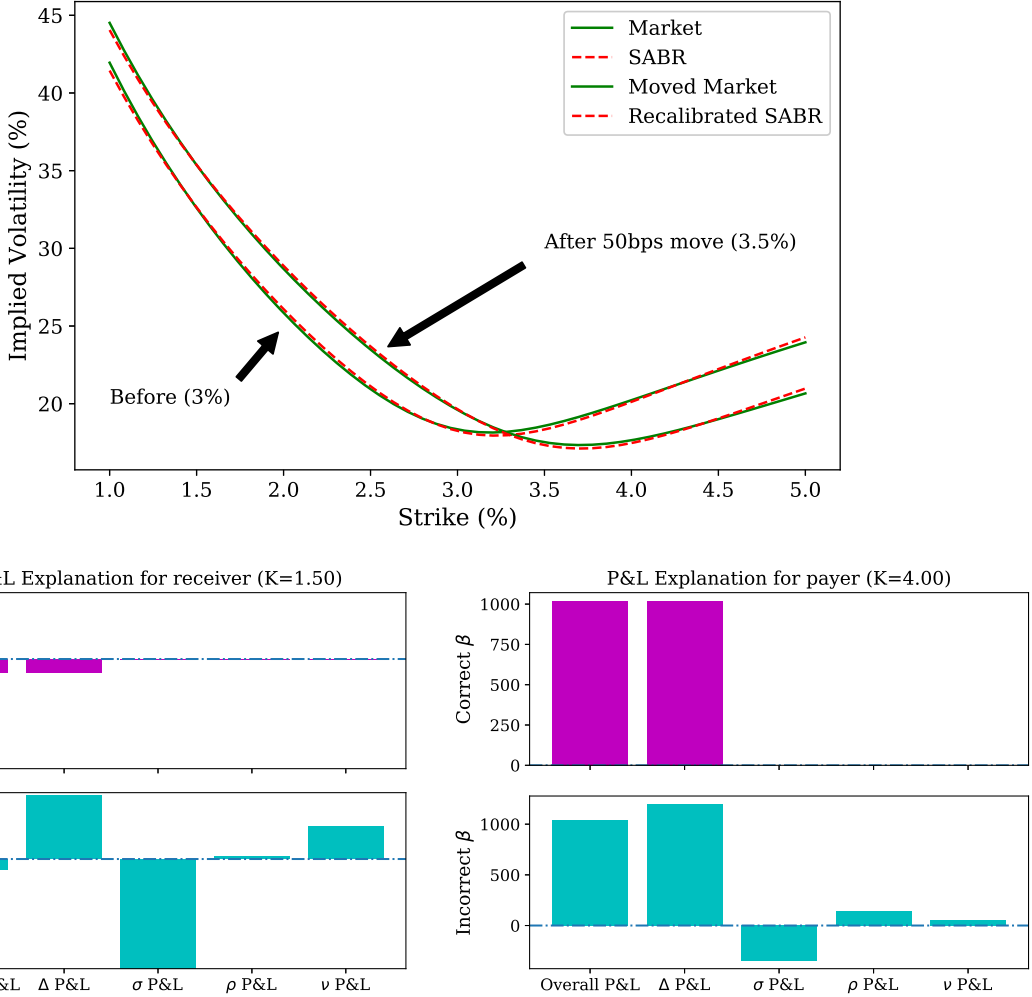
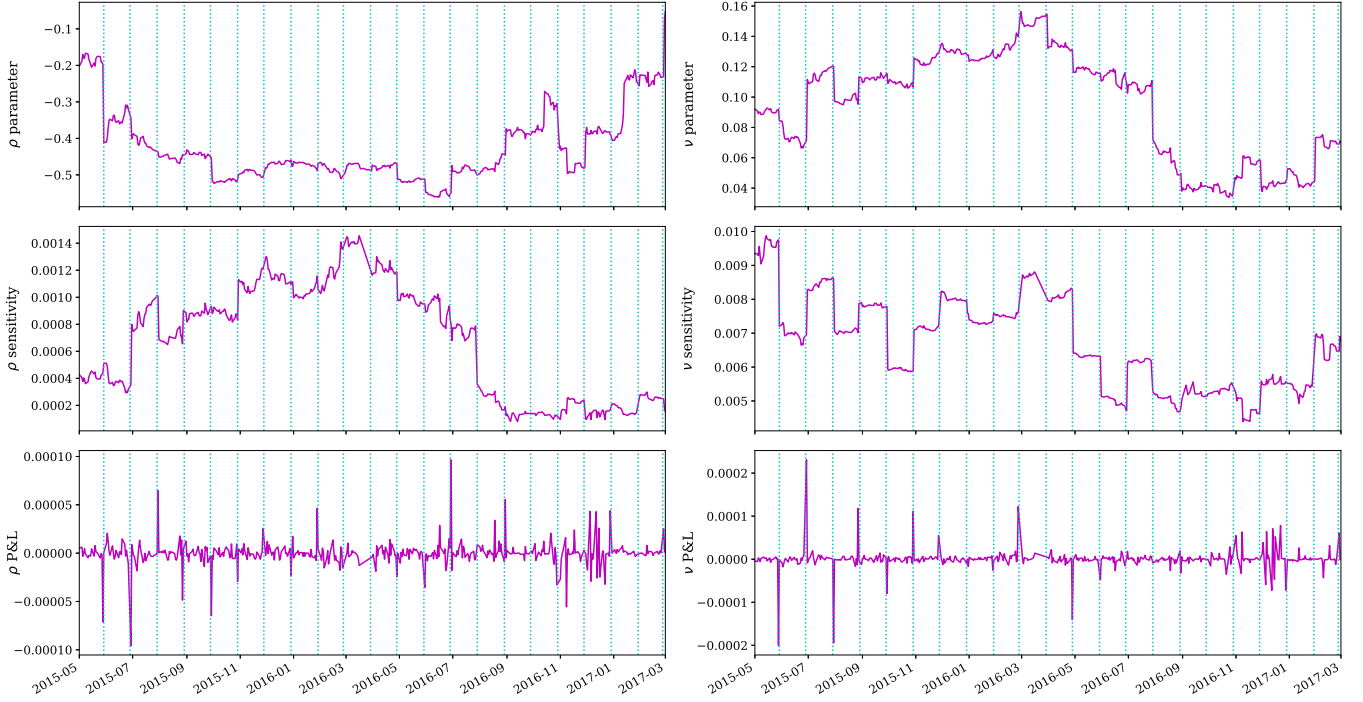


Figure 8: Comparison of SABR model's volatility backbones. The upper figure plots implied volatilities with a lognormal volatility backbone ( $\beta = 1$ ) with different forward swap rates. The defining characteristic of a lognormal backbone is that the ATM implied volatility remains at the same level when forward swap rate moves. The lower figure plots implied volatilities with a volatility backbone between normal and lognormal ( $\beta = 0.7$ ) with different forward swap rates. In this case, the ATM implied volatility decreases when forward swap rate increases, and vice versa. This behavior has important implication when it comes to efficient risk management of swaption portfolio.



**Figure 9:** Assume  $\beta_{mkt} = 0.7$ . Suppose swap rate increases, but the volatility market remains unchanged. The top figure shows the market before and after the rate increase (solid line), and the SABR model's implied volatility curve (dashed line). SABR model is able to match market well once recalibrated. The bottom figures compare the P&L explanation of an OTM receiver swaption (left figure) and an OTM payer swaption (right figure) under the “correct” and “incorrect” volatility backbone  $\beta$ . When rates increase, receiver swaption’s value decreases, while payer swaption’s value increases. Using the right backbone, the P&L of swaption holding can be explained entirely by interest rate delta, and no recalibration of model parameters is required. If the wrong backbone is used, the portfolio manager will need to recalibrate  $\alpha$ ,  $\rho$ , and  $\nu$  to match market prices again. The same P&L movement will also comprise of contribution from vega,  $\rho$  and  $\nu$  sensitivity in addition to delta.



**Figure 10:** Sensitivity of swaption portfolio to SABR model parameter. The top figures show the calibrated model parameters for  $\rho$  (skew) and  $\nu$  (smile) over a 2-year period. The dotted vertical lines highlight each month-end, when SABR parameters frequently experience jumps. The middle figures show the sensitivity of ATM swaptions to changes in  $\rho$  and  $\nu$ , i.e.  $(\frac{\partial V}{\partial \rho} \text{ and } \frac{\partial V}{\partial \nu})$  — a change in model parameters will also result in a corresponding change in model sensitivity. The bottom figures show the P&L movement of ATM swaptions over time. The frequent jumps in model parameters over month-end lead to offsetting spikes in P&L explanation as a consequence of model parameters recalibration.

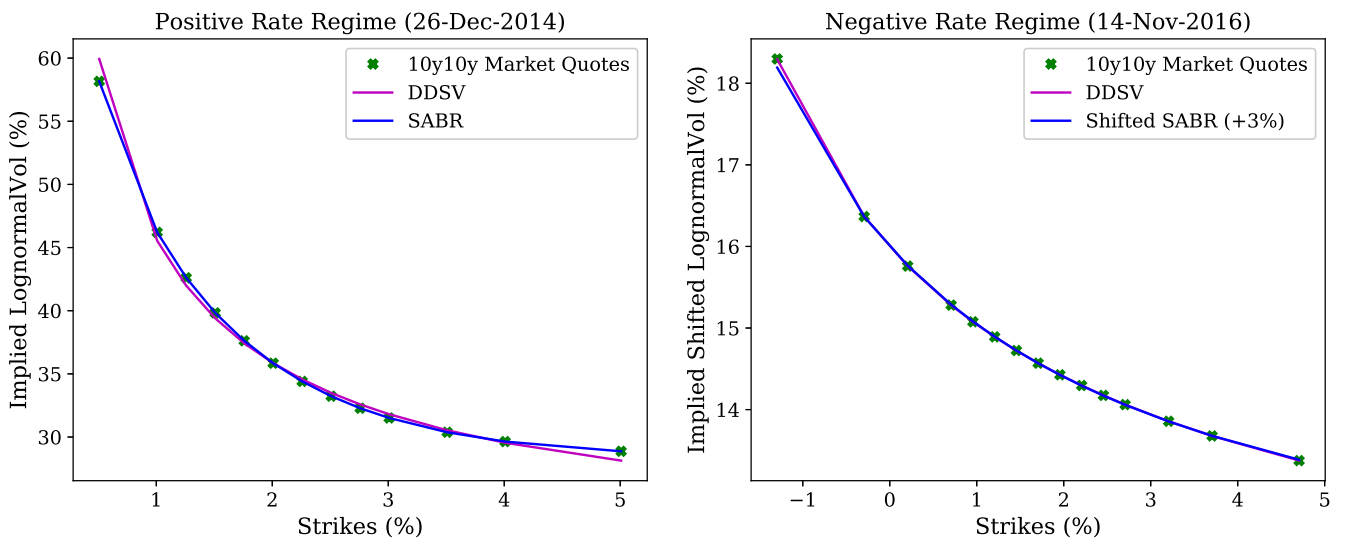


Figure 11: A comparison of SABR and DDSV models – both models are able to match observed swaption prices well once calibrated. We compare the fitting capability on a random date chosen from positive rate regime (left panel) and negative rate regime (right panel). SABR model can no longer be used once rates or strikes become negative. Market convention is to shift the rates (and strikes) up by a fixed amount before calibration. On the other hand, negative rates are admissible in the DDSV model, and it can be calibrated without any further tweaks or adjustments.

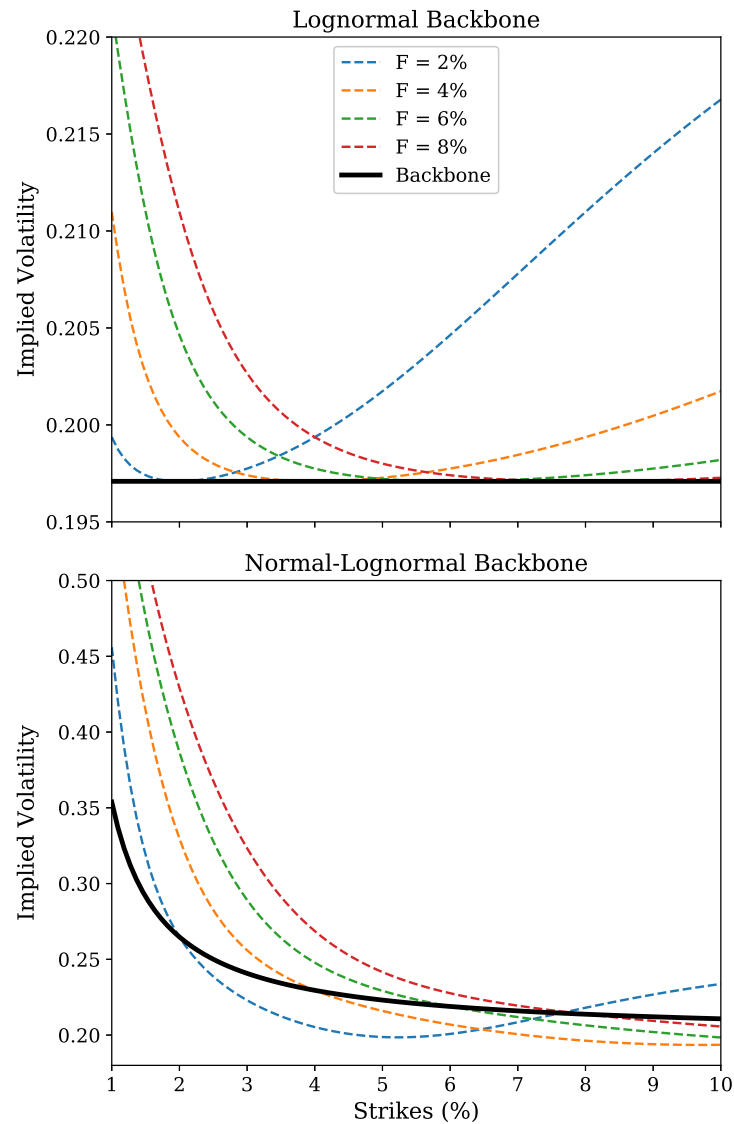
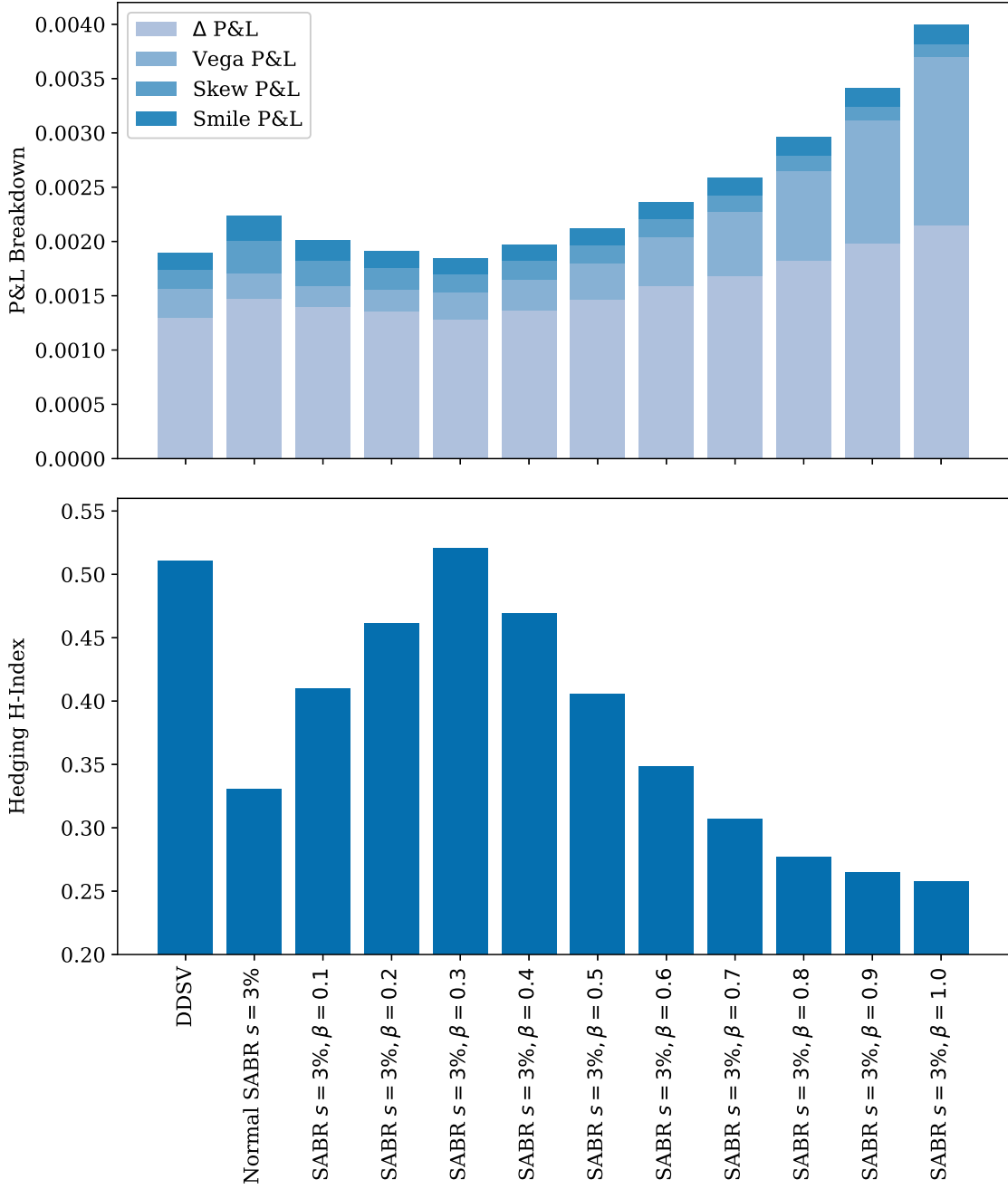
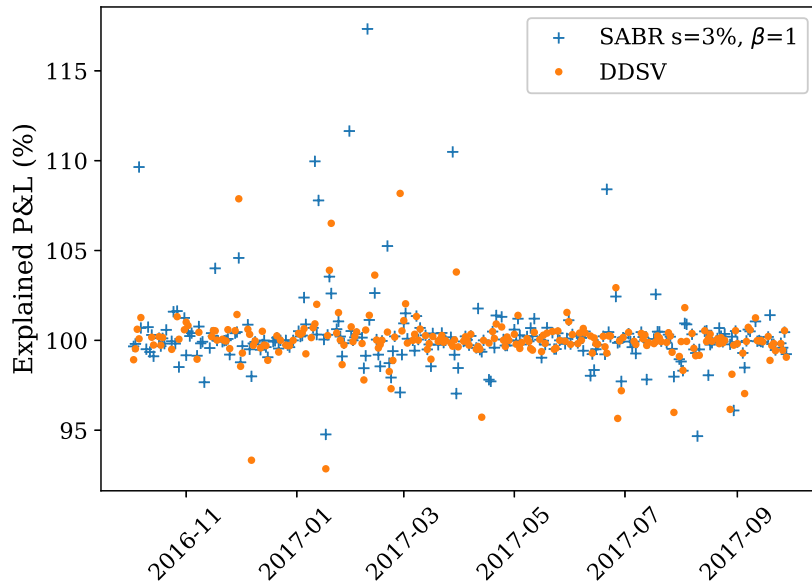


Figure 12: Comparison of DDSV model's volatility backbones. The upper figure plots implied volatilities with a lognormal volatility backbone with different forward swap rates, while the lower figure plots implied volatilities with a volatility backbone between normal and lognormal with different forward swap rates.



**Figure 13:** Comparison of hedging performance of different swaption pricing models across a 1-year period (Oct 2016 through to Sep 2017). We use a 3% shifted SABR model across different choice of  $\beta$  parameter to highlight the importance of choosing the optimal model. The upper figure shows the sum of absolute P&L breakdown in Equation 8. With the right backbone, both SABR and DDSV models are able to yield minimal hedging error and the economy of P&L explanation. The lower figure plots the Hedging Herfindahl-Hirschman index of different models. The index measures the concentration of risk in P&L explanation, and ranges from 0 to 1, with higher values indicating higher concentration in P&L explanation, which is a more desirable feature. With the right backbone, both SABR and DDSV models are again able to exhibit superior hedging performance. This is based on the assumption that over time, one major source of risk (IR Delta) would dominate, hence the economy of risk-based P&L explanation can be used as a measure to select the optimal model.



**Figure 14:** Explained P&L (in percentages) over a historical period (Oct 2016 through to Sep 2017). For comparison, we present the DDSV model along with a shifted SABR model with a  $\beta$  parameter of 1, which in our analysis is a sub-optimal model due to the inappropriate choice of volatility backbone. The Explained P&L (top figure) clearly shows that a frequently recalibrated model will generally be able to match market well, leading to close to 100% explained P&L in both cases.